Journal of Medicinal Chemistry

Article

Pharmacokinetics and metabolism of selective oxoeicosanoid (OXE) receptor antagonists and their effects on 5-oxo-6,8,11,14-eicosatetraenoic acid (5-oxo-ETE)-induced granulocyte activation in monkeys

Chantal Cossette, Shishir Chourey, Qiuji Ye, Chintam Nagendra Reddy, Vivek Gore, Sylvie Gravel, Irina Slobodchikova, Dajana Vuckovic, Joshua Rokach, and William S. Powell

J. Med. Chem., **Just Accepted Manuscript** • DOI: 10.1021/acs.jmedchem.6b00895 • Publication Date (Web): 21 Oct 2016

ACS Publications

Journal of Medicinal Chemistry is published by the American Chemical Society. 1155 Sixteenth Street N.W., Washington, DC 20036

Pharmacokinetics and metabolism of selective oxoeicosanoid (OXE) receptor antagonists and their effects on 5-oxo-6,8,11,14-eicosatetraenoic acid (5-oxo-ETE)-induced granulocyte activation in monkeys

Chantal Cossette[†‖], Shishir Chourey[‡‖], Qiuji Ye[‡], Chintam Nagendra Reddy[‡], Vivek Gore[‡⊥], Sylvie Gravel[†], Irina Slobodchikova[§], Dajana Vuckovic[§], Joshua Rokach[‡], and William S. Powell[†]*

[†]Meakins-Christie Laboratories, Centre for Translational Biology, McGill University Health Centre, 1001 Decarie Blvd, Montreal, QC H4A 3J1, Canada

[‡]Claude Pepper Institute and Department of Chemistry, Florida Institute of Technology, 150 West University Boulevard, Melbourne, FL 32901-6982, USA

[§] Department of Chemistry and Biochemistry and PERFORM Centre, Concordia University, 7141 Sherbrooke St. W., Montréal, QC H4B 1R6, Canada

[‖]These authors contributed equally to this work

[⊥]Present address for VG: Navinta LLC, 1499 Lower Ferry Rd, Ewing, New Jersey 08618-1414, USA

ABSTRACT

The potent eosinophil chemoattractant 5-oxo-6,8,11,14-eicosatetraenoic acid (5-oxo-ETE) is a 5-lipoxygenase product that acts via the selective OXE receptor, which is present in many species, but not rodents. We previously reported that the indole **230** is a potent human OXE receptor antagonist. The objective of the present study was to determine whether the monkey would be a suitable animal model to investigate its pharmaceutical potential. We found that monkey leukocytes synthesize and respond to 5-oxo-ETE, and that **230** is a potent antagonist of the OXE receptor in monkey eosinophils. Pharmacokinetic studies revealed that **230** appears rapidly in the blood following oral administration. Using chemically synthesized standards we identified the major microsomal and plasma metabolites of **230** as products of ω2-hydroxylation of the alkyl side chain. These studies demonstrate that the monkey is a promising animal model to investigate the drug potential of OXE receptor antagonists.

INTRODUCTION

5-Oxo-6,8,11,14-eicosatetraenoic acid (5-oxo-ETE) is formed by oxidation of the 5-lipoxygenase product 5S-hydroxy-6,8,11,14-eicosatetraenoic acid (5S-HETE) by 5-hydroxyeicosanoid dehydrogenase (5-HEDH) in the presence of $NADP^+$ (Fig. 1).[1] Among lipid mediators, it is the most powerful chemoattractant for human eosinophils, acting through the selective OXE receptor, which is highly expressed on eosinophils, and to a lesser extent on neutrophils.[2] Another eicosanoid derived from arachidonic acid (AA) with similar properties is prostaglandin D_2 (PGD_2), which also promotes eosinophil migration through its interaction with the DP_2 receptor, but does not elicit as strong a response as 5-oxo-ETE.[3] Leukotriene B_4 (LTB_4) is a potent chemoattractant for guinea pig eosinophils, but has only weak effects on the migration of human and monkey eosinophils,[4] its major target in humans being neutrophils.

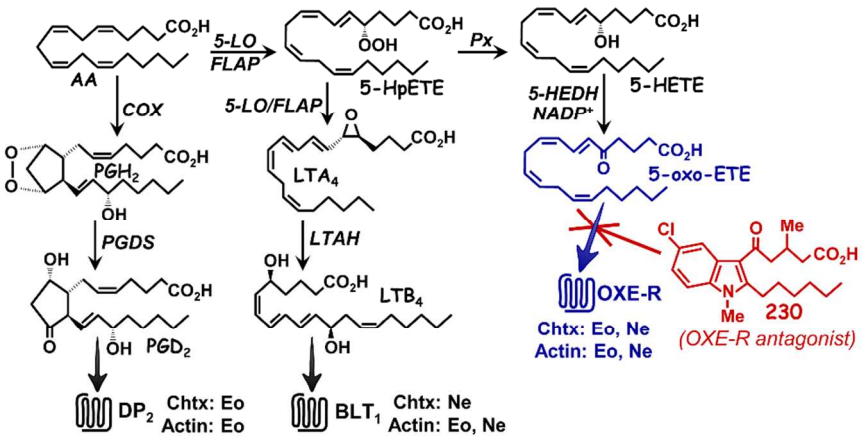

Figure 1. Synthesis of granulocyte chemoattractants from AA. AA is converted by the 5-LO pathway to LTB_4 and 5-oxo-ETE and by the cyclooxygenase (COX) pathway to PGD_2, each of which acts via its own selective receptor to induce chemotaxis (Chtx) and actin polymerization of eosinophils (Eo) and/or neutrophils (Ne). Effects mediated by the OXE receptor can be blocked by the selective antagonist **230**. Abbreviations: PGDS, PGD_2 synthase; LTAH, LTA_4 hydrolase.

Because of its potent effects on eosinophils, 5-oxo-ETE could play an important pathophysiological role in asthma and other eosinophilic diseases and for this reason we set out to develop selective OXE receptor antagonists. We recently reported two potent and selective OXE antagonists with IC_{50} values of about 30 nM in inhibiting 5-oxo-ETE-induced calcium mobilization and actin polymerization in human eosinophils and neutrophils *in vitro*. [5] Each of these compounds has a single asymmetric carbon with the antagonist activity residing almost

exclusively in the S-enantiomer, which have IC_{50} values between 5 and 10 nM.[5, 6] Testing of these OXE receptor antagonists in animal models will be required to further explore the possibility that they may be useful in treating human diseases. Although orthologs of the OXE receptor are present in many species, including zebrafish, where 5-oxo-ETE plays an important role in regulating leukocyte recruitment in response to injury, [7] there is no ortholog of this receptor in rodents. Alternative models are therefore required to test the effects of OXE antagonists. To this end we recently investigated the effects of 5-oxo-ETE on feline leukocytes and found it to be a highly potent granulocyte chemoattractant in this species. [8] However, the antagonists that we developed against the human OXE receptor were not very effective in cats, having IC_{50} values of ~5-10 μM, well over 100 times higher than those observed with human cells. Presumably differences in the sequences of the feline and human OXE receptors (76% identity) were too great to permit effective inhibition by the antagonists.

Given the above problems we decided to focus on the monkey, which has an OXE receptor ortholog that is 96% identical to the human receptor and therefore would be much more likely to respond to our antagonists than the feline receptor. Our initial objective was to determine whether monkey leukocytes can synthesize and respond to 5-oxo-ETE. Once this was accomplished we wished to determine whether 5-oxo-ETE-induced granulocyte activation could be blocked by an OXE receptor antagonist and, if so, to investigate its metabolism and pharmacokinetics to determine the suitability of the cynomolgus monkey for further *in vivo* testing. As preliminary experiments suggested that **230** (Fig. 1) is more resistant to metabolism by rat liver microsomes than the other OXE receptor antagonist that we characterized[5] we decided to initially focus on this compound for further studies in the monkey.

RESULTS

Monkey leukocytes can synthesize 5-oxo-ETE

Monkey leukocytes were incubated with 5S-HETE in the presence of phorbol myristate acetate (PMA), which triggers the respiratory burst in phagocytic cells, thus raising the intracellular levels of the 5-HEDH cofactor $NADP^+$. Analysis of the products by RP-HPLC revealed that substantial amounts of 5-oxo-ETE (t_R, 8.3 min) were synthesized under these conditions (Fig. 2A), whereas in the absence of PMA only small amounts were formed (Fig. 2A, inset). Large amounts of 5-oxo-ETE (t_R, 37.3 min) were also formed by monkey leukocytes incubated with AA in the presence of A23187 and PMA. 5S-HETE, 12S-HETE, LTB_4 and the cyclooxygenase product 12-HHT (12-hydroxy-5,8,10-heptadecatrienoic acid) were also detected (Fig. 2B). The identity of 5-oxo-ETE was confirmed by its UV spectrum (λ_{max}, 280 nm; inset to Fig. 2B).

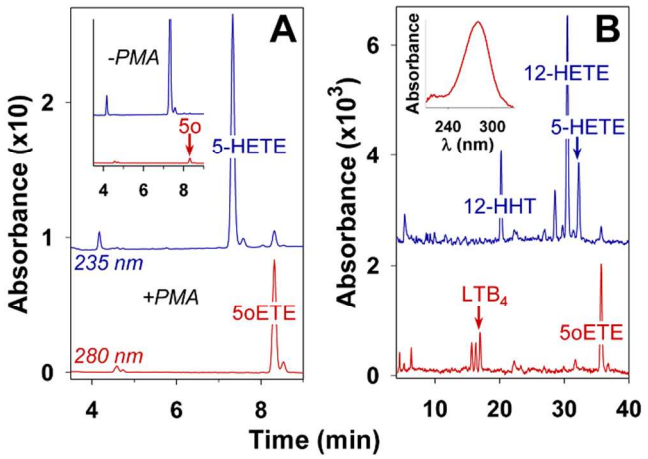

Figure 2. Biosynthesis of 5-oxo-ETE by monkey leukocytes. **A**: Monkey leukocytes (2 x 10^6 cells in 1 ml) were incubated with 5S-HETE (4 μM) for 10 min in the presence of PMA (100 nM) and the products analyzed by precolumn extraction/RP-HPLC as described in the Experimental Section. HETEs were detected at 235 nm, whereas 5-oxo-ETE (5oETE) was detected at 280 nm. The inset shows a chromatogram of the products from an identical incubation in the absence of PMA. The scale of the X-axis is the same for both chromatograms. **B**: Monkey leukocytes (2 x 10^6 cells in 1 ml) were incubated with AA (30 μM) in the presence of A23187 (5 μM) and PMA (100 nM) for 60 min and the products analyzed by RP-HPLC. The inset shows the UV spectrum of the peak labeled 5oETE with a retention time of 37.3 min. The results are representative of independent experiments using cells from 4 different monkeys.

5-Oxo-ETE elicits actin polymerization and chemotaxis in monkey leukocytes

To determine whether 5-oxo-ETE can activate monkey granulocytes, leukocytes were pretreated with APC-labeled anti-CD49d, and then exposed to agonists for 20 s. They were then treated with N-(7-nitrobenz-2-oxa-1,3-diazol-4-yl)phallacidin (NBD-phallacidin) to stain polymerized actin and analyzed by flow cytometry. Eosinophils were identified on the basis of high

expression of CD49d and high side scatter, whereas neutrophils exhibited lower CD49d expression and side scatter (Fig. 3A). We compared the effects of 5-oxo-ETE on actin polymerization to those of LTB_4 and PGD_2. 5-Oxo-ETE (EC_{50}, 1.5 ± 0.4 nM) and LTB_4 (EC_{50}, 0.7 ± 0.3 nM) had similar potencies in activating eosinophils, whereas PGD_2 (EC_{50}, 5.0 ± 1.1 nM) was somewhat less potent ($p < 0.05$; Fig. 3B). The maximal response to 5-oxo-ETE was a little higher than that to LTB_4 ($p < 0.05$). Both 5-oxo-ETE (EC_{50}, 0.9 ± 0.3 nM) and LTB_4 (EC_{50}, 0.06 ± 0.03 nM) were very active in stimulating actin polymerization in neutrophils, with LTB_4 being the more potent ($p < 0.05$; Fig. 3C). In contrast to its effects on eosinophils, PGD_2 had no measurable effect on actin polymerization in monkey neutrophils.

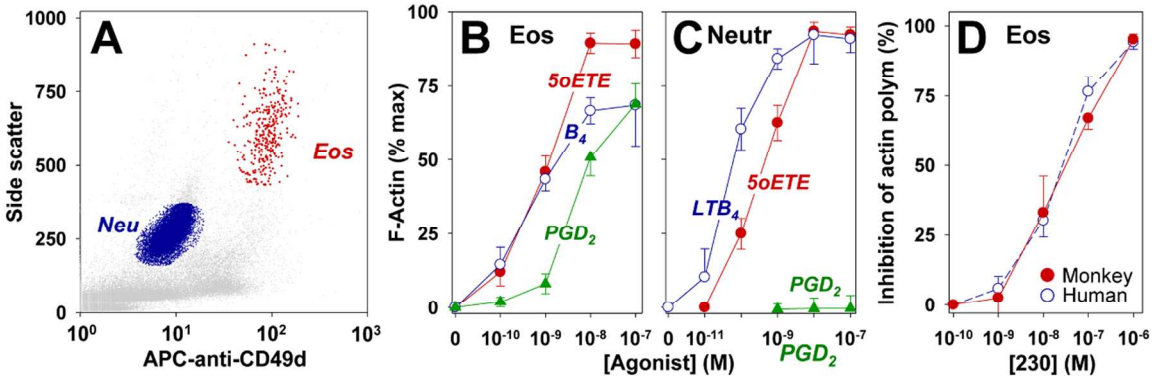

Figure 3. Effects of eicosanoids and **230** on actin polymerization in monkey granulocytes. The effects of eicosanoids on actin polymerization in eosinophils and neutrophils were evaluated by flow cytometry in APC-anti-CD49d-labeled leukocytes treated with NBD-phallacidin as described in Experimental Procedures. **A**: Dotplot showing the identification of populations of eosinophils (high side scatter and anti-CD49d labeling) and neutrophils (lower side scatter and anti-CD49d labeling). Concentration-response curves for the effects of 5-oxo-ETE (●), LTB_4 (○) and PGD_2 (▲) on actin polymerization in eosinophils (**B**) and neutrophils (**C**) were determined as described above. **D**: Leukocytes were preincubated for 5 min with different concentrations of **230** prior to the addition of 5-oxo-ETE (10 nM) and evaluation of actin polymerization as described above. Data for human granulocytes (○) taken from a previous study[5] are shown for comparison.

We also examined the effects of 5-oxo-ETE, LTB_4, and PGD_2 on leukocyte migration. Because of the limited amount of monkey blood available for these experiments we did not attempt to fractionate the leukocytes, which had been prepared by dextran sedimentation of red blood cells. These preparations contained about 39 ± 7 % neutrophils and 1.1 ± 0.2 % eosinophils. As shown

in Fig. 4A, 5-oxo-ETE and LTB_4 are potent chemoattractants for monkey leukocytes, whereas PGD_2 was virtually inactive, consistent with the predominance of neutrophils over eosinophils in these unfractionated leukocytes preparations. Although LTB_4 (EC_{50}, 2.5 ± 0.8 nM) was more potent than 5-oxo-ETE (EC_{50}, 35 ± 4 nM) ($p < 0.005$), the maximal response to 5-oxo-ETE was over 3 times greater than that to LTB_4 ($p < 0.05$).

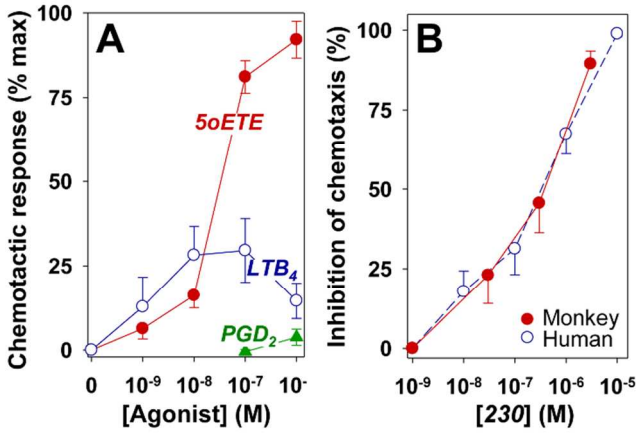

Figure 4. Effects of eicosanoids and **230** on monkey leukocyte migration. **A**: The effects of 5-oxo-ETE (●), LTB_4 (○), and PGD_2 (▲) on leukocyte migration were evaluated using microchemotaxis chambers. Vehicle or different concentrations of eicosanoids were added to the bottom chambers, whereas unfractionated leukocytes were added to the top chambers. **B**: The effects of **230** on macaque leukocyte chemotaxis (●) were evaluated as described above. **230** was added to both the top and bottom chambers. The values are means ± SE (n = 4). Data for human granulocytes (○) taken from a previous study[5] are shown for comparison.

The OXE receptor antagonist 230 is a potent inhibitor of 5-oxo-ETE-induced granulocyte activation

We found that **230** is a potent inhibitor of 5-oxo-ETE-induced actin polymerization in monkey eosinophils, with an IC_{50} of 37 ± 11 nM (Fig. 3D). The concentration-response curve for monkeys is virtually identical to that which we previously reported[5] for human eosinophils (IC_{50}, 33 ± 10 nM), which is also shown in Fig. 3D for comparison. Similarly, as shown in Fig. 4B, the effect of **230** on 5-oxo-ETE-induced leukocyte migration in monkeys (IC_{50} 422 ± 181 nM) is very similar to that for humans (454 ± 192 nM).[5] The IC_{50} values are higher for the chemotaxis assay because a higher concentration of 5-oxo-ETE (100 vs 10 nM) was employed compared to the assay for actin polymerization.

Metabolism of 230 by monkey liver microsomes

To determine the susceptibility of **230** to biological inactivation we investigated its metabolism by monkey liver microsomes. Because the presence of the 3-methyl group in the acyl side chain of **230** should block β-oxidation we initially anticipated that it would primarily be metabolized by cytochrome P450-catalyzed ω-oxidation to ω1-hydroxy and ω-carboxy metabolites (*In this paper the positions of substituents on the hexyl side chain are defined starting from the terminal methyl group, which is designated as ω1 and the adjacent methylene group as ω2, etc*). To facilitate the identification of these compounds they were chemically synthesized from the precursor 5-Cl-indole-2-carboxylic acid as shown in Scheme 1.

Scheme 1: Synthesis of ω-CO_2H-230 and ω1-OH-230[a]

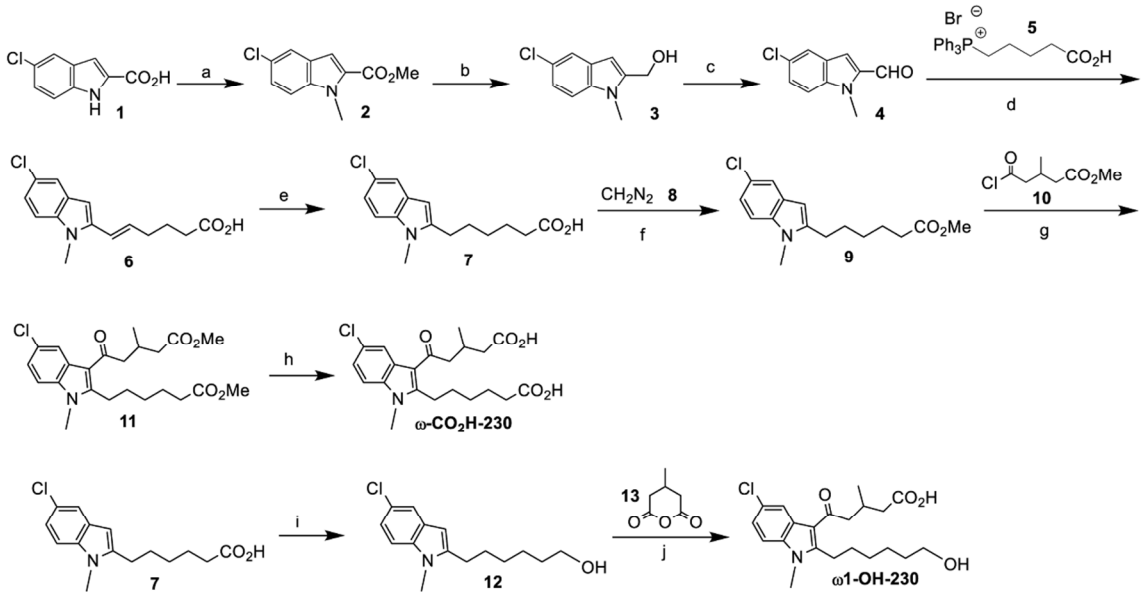

[a]**Reagents and conditions**: (a) NaH, CH_3I, DMF, 0 °C - rt, 18 h, quant; (b) $LiAlH_4$, THF, 0 °C - rt, 12 h, 86%; (c) MnO_2, CH_2Cl_2, rt, 16 h, 84%; (d) **5**, *t*BuOK, THF, –78 °C - rt, 3 h, 70%; (e) 10% Pd/C, EtOH, H_2, rt, 91%; (f) CH_2N_2, Et_2O, rt, 2 min, quant; (g) Me_2AlCl, CH_2Cl_2, **10**, CH_3NO_2, 0 °C - rt, 3 h; (h) LiOH, THF, H_2O, rt, 36 h, 50% over two steps g and h; (i) $LiAlH_4$, THF, 0 °C – rt, 14 h, 82%; (j) Me_2AlCl, CH_2Cl_2, **13**, CH_3NO_2, 0 °C – rt, 6 h, 43%.

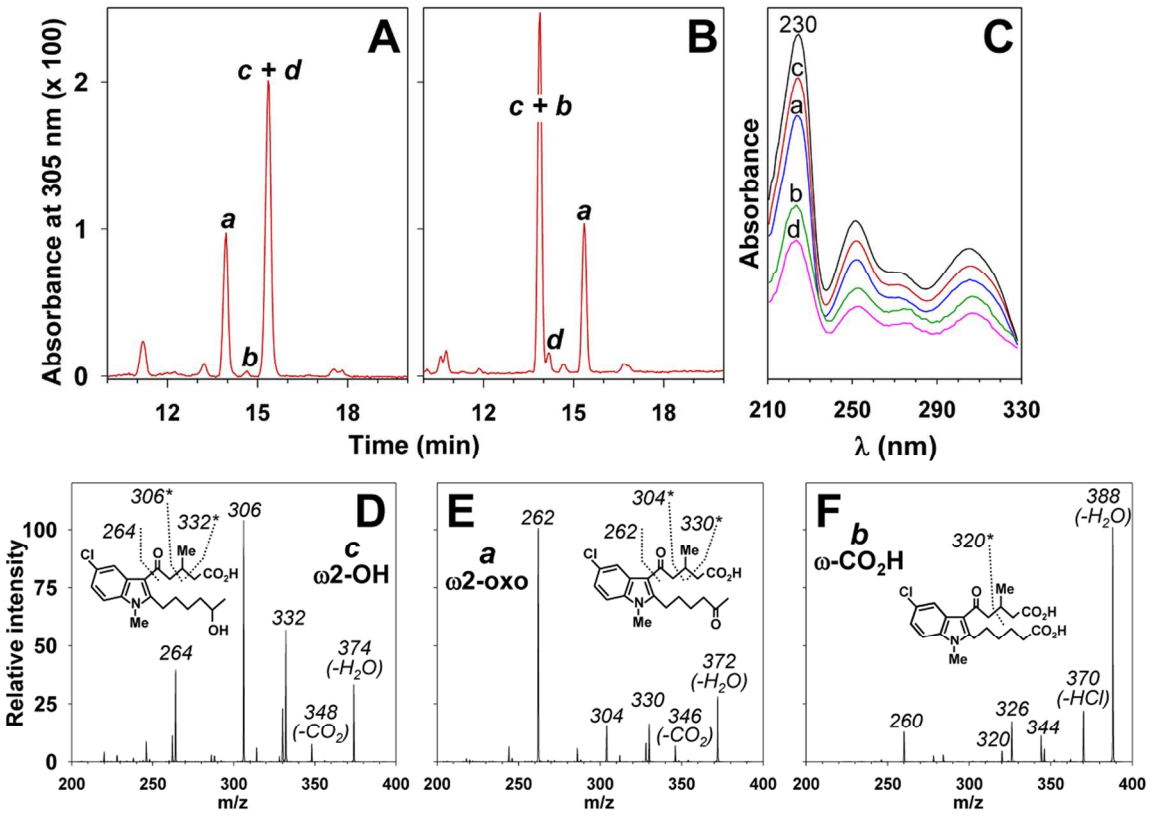

Figure 5. Metabolism of *230* by monkey liver microsomes. Monkey liver microsomes were incubated with **230** (100 µM) for 4 h in the presence of NADPH (2 mM) as described in the Experimental Section. **A**: The products were analyzed by precolumn extraction/RP-HPLC using a Novapak C18 column (4 µm particle size; 3.9 x 150 mm) with a linear gradient between 50 and 85% MeOH in H_2O containing 0.02% HOAc over 30 min at a flow rate of 1 ml/min and a temperature of 30 °C. **B**: The products were analyzed by precolumn extraction/RP-HPLC using a Kinetex C18 column (2.6 µm particle size; 4.6 x 100 mm) with a linear gradient between 30 and 65% MeCN in H_2O containing 0.02% HOAc over 35 min at a flow rate of 1 ml/min and a temperature of 30 °C. **C**: UV spectra of the major metabolites of **230** obtained using a diode array UV detector. All spectra were from the MeOH/H_2O gradient except for ω-hydroxy-**230** (***d***) which was from the MeCN/H_2O gradient. The scale of the Y-axis was adjusted for each of the spectra to facilitate comparison. **D-F**: Collision-induced dissociation of the $[M-H]^-$ ions of (**D**) metabolite ***c*** (m/z 392.1612) in panel B, (**E**) metabolite ***a*** (m/z 390.1478) and (**F**) metabolite ***b*** (m/z 406.1402). * Ions that are formed as a result of a McLafferty rearrangement.

The products formed after incubation of **230** (50 µM) with monkey liver microsomes (0.8 mg protein/mL) in the presence of NADPH (2 mM) for 4 h were analyzed by RP-HPLC using a water/methanol gradient (Fig. 5A). Two major products with retention times of 13.95 min (***a***) and 15.35 min (***c***) were detected. Metabolite ***c*** cochromatographed with authentic ω1-hydroxy-**230** (data not shown), whereas metabolite ***a*** had a retention time somewhat lower than that of authentic ω-carboxy-**230**, which cochromatographed with the minor product (***b***) of intermediate

polarity (t_R, 14.65 min). When we repeated the analysis using a water/acetonitrile gradient the order of elution of the two major metabolites was reversed (Fig. 5B). Under these conditions, ***c*** (t_R, 13.88 min) no longer cochromatographed with ω1-hydroxy-**230**, but instead cochromatographed with the minor product ***b***. With the acetonitrile gradient the minor product ***d*** (t_R, 14.18 min) cochromatographed with authentic ω1-hydroxy-**230** (not shown), whereas the major product ***a*** (t_R, 15.35 min) had a considerably longer retention time.

Scheme 2. Synthesis of ω2-OH-230 and ω2-oxo-230[a]

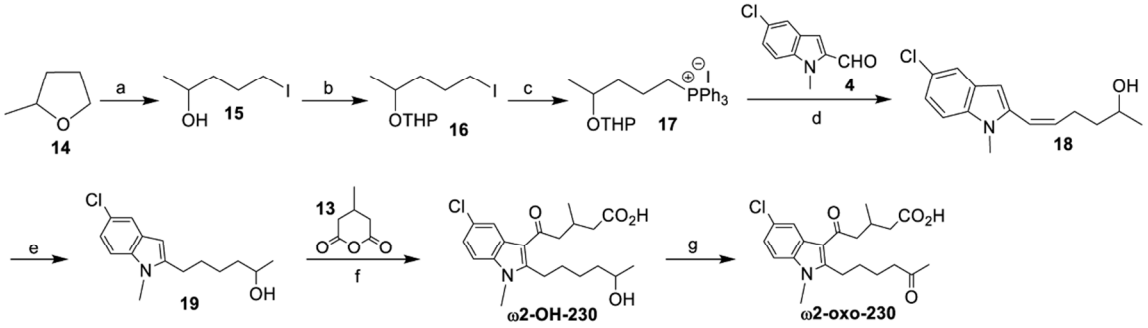

[a]**Reagents and conditions**: (a) $Et_4N^+I^-$, BF_3-Et_2O, CH_2Cl_2, rt, 48%; (b) DHP, PPTS, THF, rt, 90%; (c) PPh_3, CH_3CN, 85 °C, 47 h; (d) KHMDS, –78 °C - 0 °C, 3 h, aq. NH_4Cl solution, 58%; (e) 10% Pd/C, EtOH, H_2, rt, 3 h, quant; (f) Me_2AlCl, 13, CH_3NO_2, rt, 3 h, 82%; (g) DMP, CH_2Cl_2, rt, 9 h, 64%.

The reversal in the order of elution of ***a*** and ***c*** in a water/methanol vs a water/acetonitrile gradient is characteristic of a pair of compounds that differ from one another by an oxo vs a hydroxyl group.[9] We therefore postulated that **230** is metabolized by ω-1 oxidation (i.e. oxidation of the ω2 methylene group) to give ω2-hydroxy-**230** and ω2-oxo-**230**. To aid in the identification of these products the authentic compounds were prepared by chemical synthesis as shown in Scheme 2. Metabolites ***a*** and ***c*** cochromatographed with authentic ω2-oxo-**230** and ω2-hydroxy-**230**, respectively, in both methanol/water and acetonitrile/water gradients (data not shown). The UV spectra of compounds ***a*** - ***d*** (Fig. 5C) were all virtually identical to that of **230**, consistent with an unaltered indole chromophore and modification of one of the side chains. Further support for the above structural assignments was obtained by LC/MS/MS analysis. Metabolites ***c***

and ***d*** had $[M-H]^-$ ions at m/z 392.1612 and 392.1611, respectively, compared to the theoretical value m/z 392.1634 for a monohydroxy metabolite of **230** (mass accuracy, 5.6 ppm). The MS^2 fragmentation pattern of the $[M-H]^-$ ion for ***c*** (Fig. 5D) is identical to that of authentic ω2-hydroxy-**230** (not shown), with major ions at m/z 374 (loss of H_2O), 348 (loss of CO_2), 332 (loss of $CH_2C(OH)_2$ due to a McLafferty rearrangement), 306 (loss of CH_2=CH-CH_2-CO_2H due to a different McLafferty rearrangement), and 264 (loss of the acyl side chain).

Metabolite ***a*** had an $[M-H]^-$ ion at m/z 390.1457, compared to the theoretical value of 390.1478 expected for ω2-oxo-**230** (mass accuracy, 5.4 ppm). Furthermore, the MS^2 fragmentation pattern of the $[M-H]^-$ ion from ***a*** (Fig. 5E) is identical to that of authentic ω2-oxo-**230** (not shown) and was similar to that of ω2-hydroxy-**230** except that the m/z values of the major ions were 2 mass units lower: 372 (loss of H_2O), 346 (loss of CO_2), 330 (loss of $CH_2C(OH)_2$ due to a McLafferty rearrangement), 304 (loss of CH_2=CH-CH_2-CO_2H due to a McLafferty rearrangement), and 262 (loss of the acyl side chain).

The mass spectrum of ***d*** was very similar to that of ***c*** and identical to that of authentic ω1-hydroxy-**230** (data not shown). There was also another metabolite with a t_R (14.65 min) between those of ***d*** and ***a*** (Fig. 5B) with an almost identical mass spectrum (not shown), indicating that it is a regioisomer of these compounds with the hydroxyl group at a different position in the hexyl side chain.

Finally, the m/z value for the $[M-H]^-$ ion of metabolite ***b*** was 406.1402, compared to the theoretical value of 406.1427 for ω-carboxy-**230** (mass accuracy, 6.2 ppm). The MS^2

fragmentation pattern of this metabolite (Fig. 5F) is identical to that of authentic ω-carboxy-**230** (not shown) with prominent ions with m/z values of 388 (loss of H_2O), 370 (loss of HCl), 344 (loss of H_2O and CO_2), 326, 320 (loss of CH_2=CH-CH_2-CO_2H due to a McLafferty rearrangement), and 260.

Scheme 3: Synthesis of 197 and 225[a]

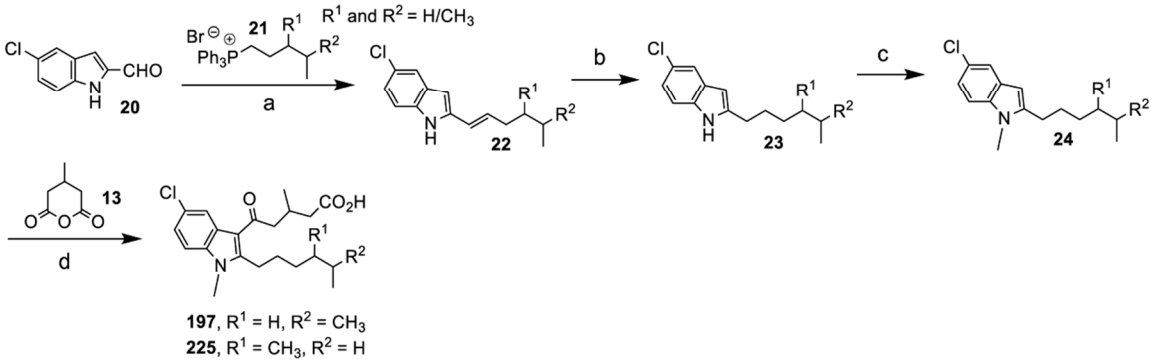

[a]**Reagents and conditions**: (a) **21**, LiHMDS, −78 °C - 0 °C, 3 h, 90%; (b) 10% Pd/C, EtOH, H_2, rt, 3 h, 91%; (c) KOH, DMSO, CH_3I, rt, 3 h, 95%; (d) Me_2AlCl, CH_2Cl_2, **13**, rt, 3 h, 64%.

Effects of a branched-chain alkyl group on antagonist potency

We attempted to reduce the metabolism of our OXE antagonist by replacing the hexyl group with a branched-chain alkyl group, which we hoped would be more resistant to ω-oxidation. To this end we synthesized compounds **197** and **225**, in which the hexyl group of **230** is replaced by a 5-methylhexyl or a 4-methylhexyl group, respectively (Scheme 3). Both compounds were prepared from the precursor 5-chloroindole-2-carbaldehyde as shown in Scheme 3. The effects of these compounds on 5-oxo-ETE-induced calcium mobilization in human granulocytes are shown in Fig. 6. The concentration-response curve for **197** (IC_{50}, 20 ± 6 nM) is nearly identical to that for **230** (IC_{50}, 16 ± 4 nM), whereas **225** (IC_{50}, 88 ± 26 nM) is over 4 times less potent.

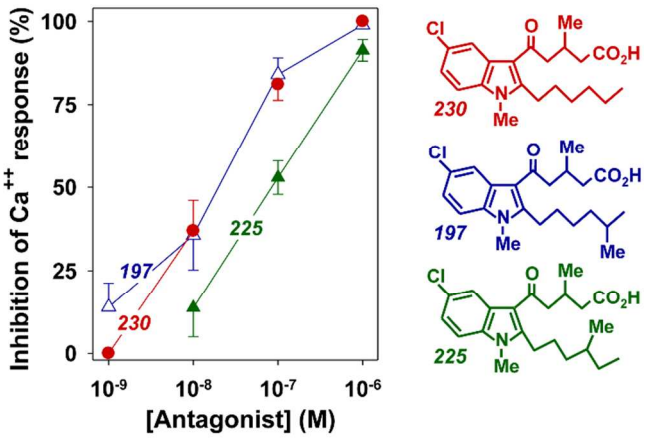

Figure 6. Effects on antagonist potency of adding a methyl group to the hexyl side chain of **230.** Calcium mobilization was measured in human neutrophils stimulated with 10 nM 5-oxo-ETE following the addition of either vehicle, **230** (●), **197** (Δ), or **225** (▲). All compounds were racemic mixtures.

Metabolism of 197 by monkey liver microsomes

Because **197** is the more potent of the above two branched chain compounds we further investigated its metabolism. **197** (50 μM) was incubated with monkey liver microsomes in the presence of NADPH for 4 h and the products were analyzed by RP-HPLC using a water/acetonitrile gradient. Under these conditions **197** was almost completely converted to two major metabolites, ***x*** (t_R, 13.69 min) and ***y*** (t_R, 23.69 min), along with several minor metabolites (Fig. 7A). Analysis of the same sample using a water/methanol gradient gave a very similar distribution of peaks (data not shown), with no apparent change in the order of elution. As with the major microsomal metabolites of **230**, both ***x*** and ***y*** had UV spectra virtually identical to that of **197**, suggesting that the indole chromophore had not been altered (Fig. 7B).

Analysis by LC-MS revealed that the $[M-H]^-$ ion of metabolite ***y*** has an m/z value of 406.1769, within 3.9 ppm of the theoretical value of 406.1785 for a monohydroxy metabolite of **197**. The MS^2 fragmentation pattern of ***y*** (Fig. 7C) was dominated by fragmentation of the acyl side chain and exhibited major ions at m/z 388 (loss of H_2O), 362 (loss of CO_2), 346 (loss of $CH_2C(OH)_2$ due to a McLafferty rearrangement), 320 (base peak; loss of CH_2=CH-CH_2-CO_2H due to a McLafferty rearrangement), and 278 (loss of the acyl side chain). Since the UV and MS^2 spectra

of this compound rule out alterations involving the indole and acyl side chain, respectively, it can be concluded that the additional hydroxyl group in metabolite ***y*** is located on the alkyl side chain.

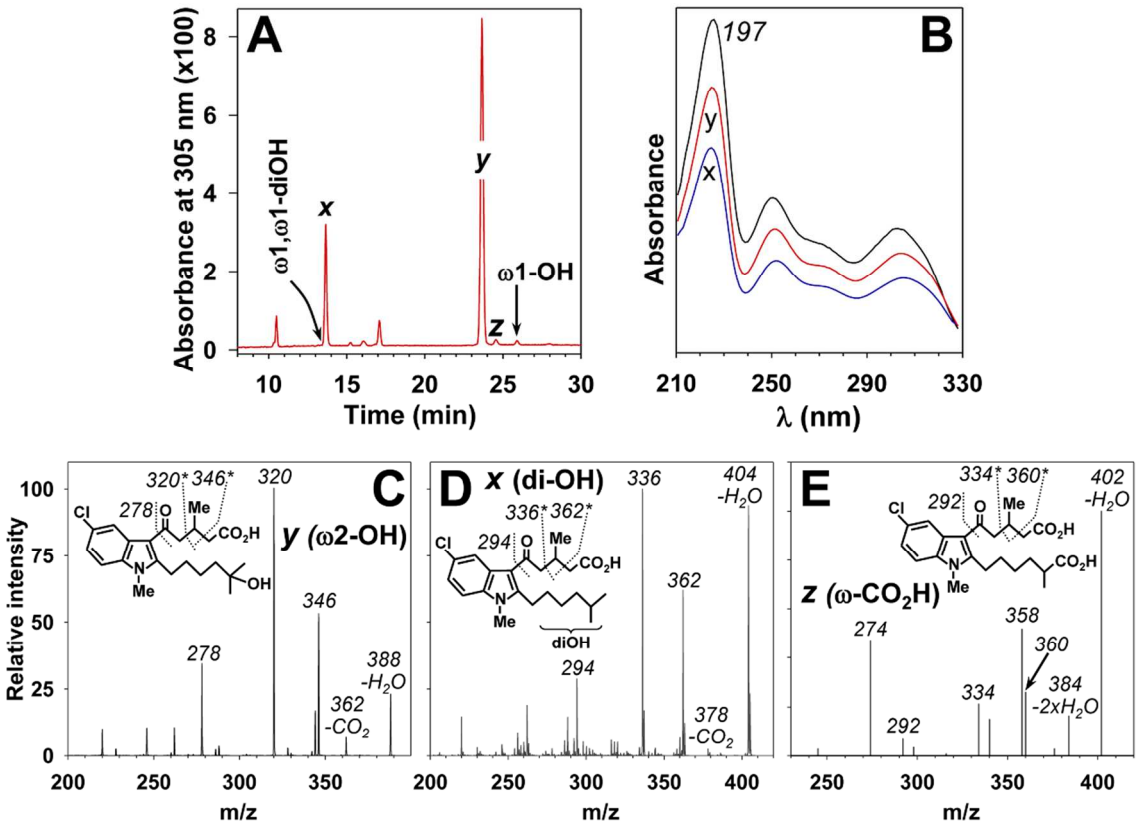

Figure 7. Metabolism of *197* by monkey liver microsomes. Monkey liver microsomes were incubated with *197* (100 μM) for 4 h in the presence of NADPH (2 mM) as described in the Experimental Section. **A**: The products were analyzed by precolumn extraction/HPLC using a Kinetex C18 column (5 μm particle size; 4.6 x 250 mm) with a linear gradient between 30 and 65% MeCN in H_2O containing 0.02% HOAc over 35 min at a flow rate of 1 ml/min and a temperature of 35 °C. **B**: UV spectra of the major metabolites of *197* obtained using a diode array UV detector. The scale of the Y-axis was adjusted for each of the spectra to facilitate comparison. **C-E**: Collision-induced dissociation of the $[M-H]^-$ ions of (**C**) metabolite ***y*** (m/z 406.1769), (**D**) metabolite ***x*** (m/z 422.1721), and (**E**) metabolite *z* (m/z 420.1578). * Ions that are formed as a result of a McLafferty rearrangement.

The second major metabolite (***x***; t_R, 13.69 min) has an $[M-H]^-$ ion with an m/z of 422.1721, which is within 3.1 ppm of the theoretical value of 422.1734 expected for a dihydroxy metabolite. The MS^2 fragmentation pattern of this compound (Fig. 7D) has fragment ions with m/z values of 404 (loss of H_2O), 378 (loss of CO_2), 362 (loss of $CH_2C(OH)_2$ due to a McLafferty

rearrangement), 336 (base peak; loss of CH_2=CH-CH_2-CO_2H due to a McLafferty rearrangement), and 294 (loss of the acyl side chain). The UV spectrum of ***x***, combined with its mass spectrum containing a prominent McLafferty rearrangement-derived ion emanating from loss of the major part of the acyl side chain, suggest that both hydroxyl groups are situated on the alkyl side chain.

Scheme 4: Synthesis of ω1-OH-197[a]

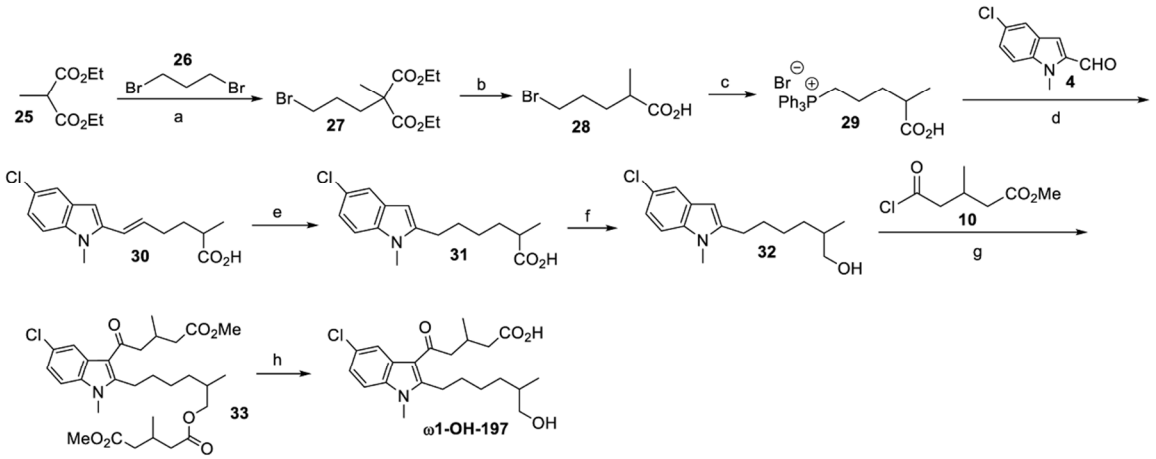

[a]**Reagents and conditions**: (a) NaH, DMF, 0 °C - rt, 2 h, 70%; (b) HBr, Ac_2O, reflux, 16 h, 72%; (c) PPh_3, CH_3CN, reflux, 18 h, 70%; (d) *t*BuOK, −10 °C - 0 °C, 3 h, 57%; (e) 10% Pd/C, H_2, EtOH, rt, 98%; (f) $LiAlH_4$, THF, −20 °C - rt, 4 h, 67%; (g) Me_2AlCl, CH_2Cl_2, **10**, CH_3NO_2, 0 °C - rt, 3 h, 70%; (h) LiOH, THF, H_2O, rt, 48 h, 70%.

Scheme 5: Synthesis of ω2-OH-197[a]

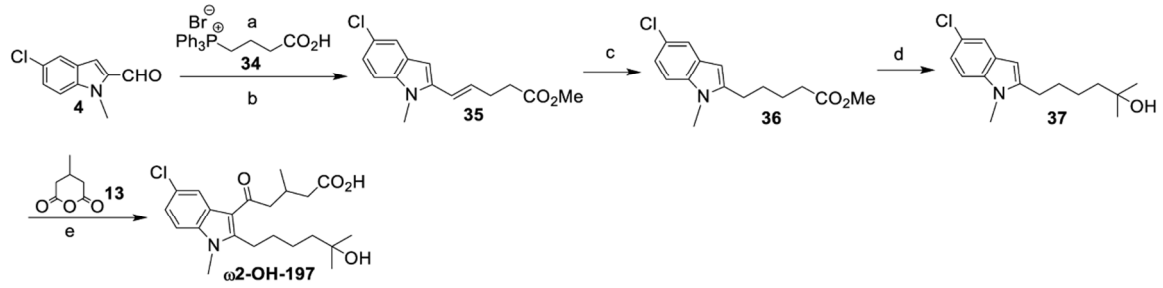

[a]**Reagents and conditions**: (a) **34**, *t*BuOK, THF, −78 °C - rt, 3 h; (b) KOH, DMSO, CH_3I, rt, 3 h, 85% over steps a and b; (c) 10% Pd/C, benzene, H_2, rt, 3 h, 98%; (d) CH_3MgBr, THF, 0 °C – rt, 30 min, 85%; (e) Me_2AlCl, CH_2Cl_2, **13**, rt, 3 h, 54%.

Since it was not possible to determine the precise positions of the hydroxyl groups in ***x*** and ***y*** from the above mass spectral data we prepared several potential candidates by total chemical synthesis. The first of these, ω1-OH-**197**, was prepared as shown in Scheme 4. However, this compound did not cochromatograph with the major metabolite ***y***, but rather with a minor product with a t_R of 25.92 min (Fig. 7A), the identity of which was confirmed to be ω1-OH-**197** based on the identity of the MS^2 fragmentation pattern of its $[M-H]^-$ ion with that of the authentic standard (not shown). We then prepared ω2-OH-**197** as shown in Scheme 5. This compound cochromatographed with ***y*** and had an MS^2 fragmentation pattern identical to that shown in Fig. 7C for the microsomal metabolite, confirming the identity of metabolite ***y*** as ω2-OH-**197**.

Scheme 6: Synthesis of ω1,ω1-diOH-197[a]

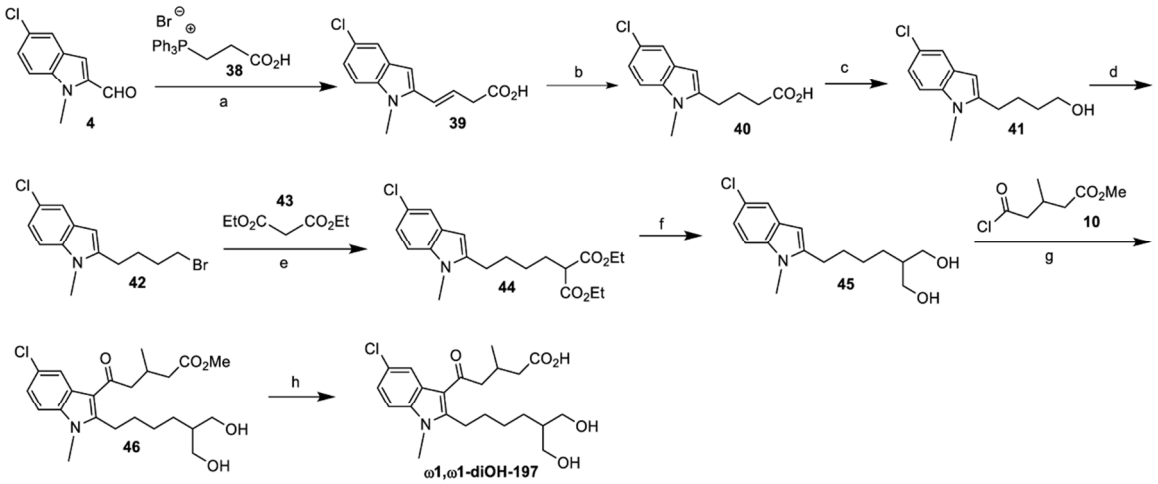

[a]**Reagents and conditions**: (a) **38**, *t*BuOK, CH_2Cl_2, THF, −78 °C - rt, 5 h; (b) Pd/C, EtOAc, 6 h, rt, 73% over two steps; (c) $LiAlH_4$, THF, 0 °C - rt, 30 min, 83%; (d) CBr_4, PPh_3, CH_2Cl_2, rt, 1 h, 94%; (e) **43**, NaH, 0 °C - rt, 14 h, 74%; (f) $LiAlH_4$, THF, 0 °C - rt, 4 h, 81%; (g) Me_2AlCl, CH_2Cl_2, **10**, 0 °C - rt, 45 min; (h) LiOH, THF, H_2O, rt, 22 h, 59% over two steps g and h.

In an attempt to identify the dihydroxy metabolite of **197** we prepared ω1,ω1-diOH-**197**, by total chemical synthesis as shown in Scheme 6. However, this compound had a t_R (13.46 min), slightly lower than that of metabolite ***x*** (t_R, 13.65 min), consistent with ***x*** being an isomeric dihydroxy metabolite, possibly ω1,ω2-diOH-**197** or ω2,ω3-diOH-**197**.

The mass spectrum of another minor product (*z*; t_R 24.56) exhibited an $[M-H]^-$ ion at m/z 420.1578, indicative of an ω-carboxy metabolite (i.e. ω-CO_2H-**197**). The MS^2 fragmentation pattern derived from this ion (Fig. 7E) gave fragment ions at m/z 402 (base peak; loss of H_2O), 384 (loss of 2 molecules of H_2O), 360 (loss of $CH_2C(OH)_2$ due to a McLafferty rearrangement), 358 (loss of H_2O and CO_2), 334 (loss of $–CH_2=CH-CH_2-CO_2H$ due to a McLafferty rearrangement), 292 (loss of acyl side chain), and 274 (loss of acyl side chain + H_2O).

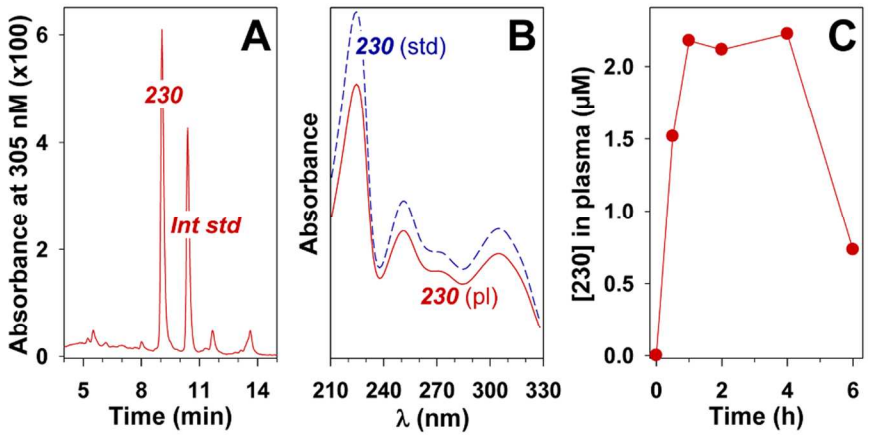

Figure 8. *In vivo* metabolism of **230** in rats. **230** was administered by oral gavage to rats as described in Materials and Methods. The rats were sacrificed after different times and plasma samples were analyzed by RP-HPLC following solid-phase extraction using **197** as an internal standard as described in the Experimental Section. **A**: Chromatogram of an extract of plasma obtained 4 h after administration of **230** (30 mg/kg). B: UV spectra of the peak labeled "**230**" in panel A and authentic **230**. C: Plasma levels of **230** after oral administration of a dose of 30 mg/kg. Each point represents a single rat (blood was taken only once at the time the animal was sacrificed).

Pharmacokinetics of 230 in rats

We conducted a pilot study in rats to determine whether **230** would appear in the blood after oral administration. **230** (30 mg/kg) was administered by oral gavage and the animals were sacrificed after different time points. Only a single blood sample was taken by cardiac puncture from each rat at the end of the experiment. Plasma samples were analyzed by RP-HPLC following solid-phase extraction, using **197** as an internal standard. Considerable amounts of **230** were detected in plasma after 4 h, with only relatively minor peaks containing potential metabolites being

detected (Fig. 8A). The identity of **230** was confirmed by its retention time and UV spectrum (Fig. 8B). **230** rapidly appeared in the blood and was detected at a level of about 1.5 μM after 30 min (Fig. 8C). The plasma concentration rose to about 2.2 μM between 1 and 4 h and then declined to about 0.7 μM at 6 h, which was the longest time investigated. No adverse effects of **230** on the rats were observed prior to sacrifice at the end of the experiment.

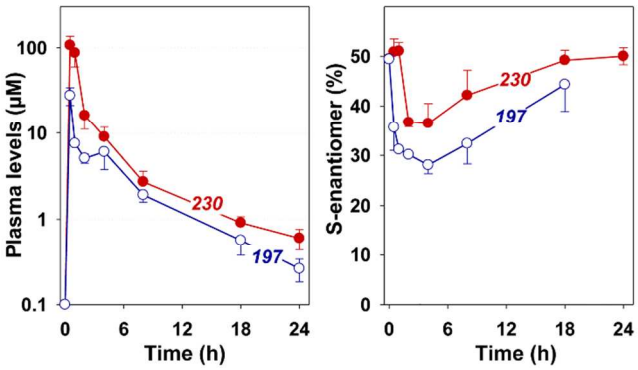

Figure 9. Pharmacokinetics of **230** and **197** in monkeys. A: **230** (●; n = 4) and **197** (○; n = 2) were administered by oral gavage to cynomolgous monkeys as described in Materials and Methods. Plasma was prepared from blood samples taken immediately before and 0.5, 1, 2, 4, 8, 18, and 24 h after administration of antagonist. After solid-phase extraction the samples were analyzed by precolumn extraction/RP-HPLC using **197** as an internal standard in the case of **230** and **230** as an internal standard for analysis of plasma levels of **197**. B: The peaks for **230** (●) and **197** (○) obtained after RP-HPLC of plasma samples were collected and subjected to chiral-HPLC to determine the proportions of R- and S-enantiomers.

Pharmacokinetics of 230 and 197 in monkeys

We next performed more extensive experiments in cynomolgus monkeys to investigate the pharmacokinetics and metabolism of **230**. The levels of **230** were analyzed as described above in plasma samples obtained over a period of 24 h following administration by oral gavage. As in rats, **230** appeared very rapidly in plasma, but the levels were much higher in monkeys, reaching maximal concentrations of about 100 μM by 30 min and subsequently declining to 2.7 μM by 8 h and to about 0.6 μM at 24 h (Fig, 9A). We also examined the pharmacokinetic profile of **197** and found it to be similar to that of **230**, except that the plasma concentrations were somewhat lower (Fig. 9A). A maximum concentration of **197** of about 30 μM was reached by 30 min, which declined to about 2 μM by 8 h and 0.3 μM at 24 h. As both **230** and **197** are racemates, we collected fractions containing the unmetabolized compounds after RP-HPLC and determined the

relative amounts of R and S enantiomers by chiral HPLC. In both cases there was a marked predominance of the R enantiomers at time points up to 8 h, after which time the ratio of R:S declined to approach the starting ratio of about 1:1 by 18 h (Fig. 9B).

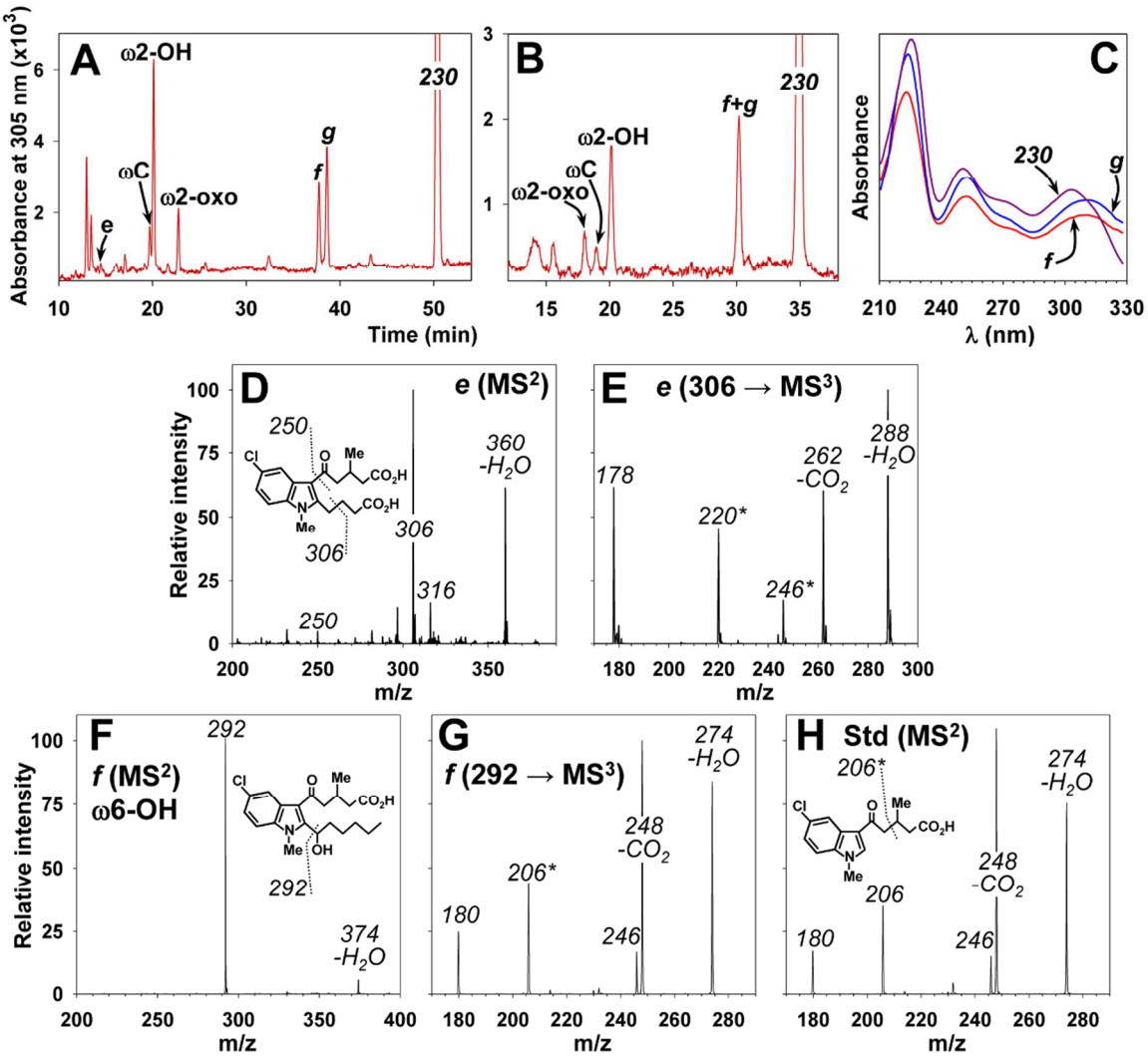

Figure 10. *In vivo* metabolism of **230** in monkeys. **230** was administered by oral gavage to a cynomolgus monkey as described in the Experimental Section and plasma was prepared from a blood sample taken after 4 h. After solid-phase extraction the sample was analyzed either by RP-HPLC using a UV detector or by LC-MS. **A**: RP-HPLC of an aliquot of a plasma extract on a Kinetex C18 column (5 µm particle size; 4.6 x 250 mm) using a gradient between 35 and 65% MeCN in water containing 0.02% HOAc over 60 min with a flow rate of 1 ml/min and a temperature of 35 °C. **B**: RP-HPLC of an aliquot of a plasma extract on a Novapak C18 column (4 µm particle size; 150 x 3.9 mm) using a gradient between 50 and 80% MeOH in water containing 0.02% HOAc over 40 min with a flow rate of 1 ml/min and a temperature of 30 °C. **C**: UV spectra of **230** and metabolites *f* and *g*. The scale of the Y-axis was adjusted for each of the spectra to facilitate comparison. **D**: Collision-induced dissociation of the $[M-H]^-$ ion (m/z 378) of metabolite *e*. **E**: MS^3 spectrum showing daughter ions derived from the fragment ion of *e* at m/z 306 shown in panel **D**. **F**: Collision-induced dissociation of the $[M-H]^-$ ion (m/z 392) for metabolite *e*. **G**: MS^3 spectrum showing daughter ions resulting from collision-induced dissociation of the ion at m/z 292 in the mass spectrum of *f* shown in panel F. **H**: Collision-induced dissociation of the $[M-H]^-$ ion (m/z 292) of the authentic standard **51** lacking the alkyl side chain. * Ions that are formed as a result of a

McLafferty rearrangement.

In vivo metabolism of 230 in monkeys

The *in vivo* metabolism of **230** was investigated using RP-HPLC with UV detection as well as by LC-MS. The HPLC profile of UV-absorbing peaks in a plasma sample taken 4 h after administration of **230** using a water/acetonitrile gradient as the mobile phase is shown in Fig. 10A. As was he case with monkey liver microsomes, the major polar metabolite was identified as ω2-OH-**230** (t_R, 20.13 min) by cochromatography with the authentic standard. Smaller amounts of ω-carboxy-**230** (t_R, 19.70 min) and ω2-oxo-**230** (t_R, 22.79 min) were also identified by cochromatography with authentic standards. When a water/methanol gradient was used (Fig. 10B) the elution order changed, with ω2-oxo-**230** having the shortest t_R (18.0 min) of the above three products, followed by ω-carboxy-**230** (t_R, 18.9 min) and ω2-OH-**230** (t_R, 20.1 min). The identity of each of the above three plasma metabolites was confirmed by LC-MS analysis, with the exact masses of the M-H ions and the MS^2 spectra being identical to those of the authentic standards (data not shown). We also detected a small amount of a more polar product (***e***; t_R, 14.16 min in Fig. 10A), which cochromatographed with authentic ω-carboxy-dinor-**230**, synthesized as shown in Scheme 7. Metabolite ***e*** has an $[M-H]^-$ ion at m/z 378.1113, within 1.3 ppm of the theoretical value expected for ω-carboxy-dinor-**230** (378.1108), and its MS^2 fragmentation pattern (Fig. 10D) matched that of the authentic compound, with major ions at m/z 360 (loss of H_2O), 316 (loss of H_2O and CO_2), 306 (loss of CH_2=CH-CO_2H) and 250 (loss of

Scheme 7: Synthesis of dinor-ω-CO_2H-230[a]

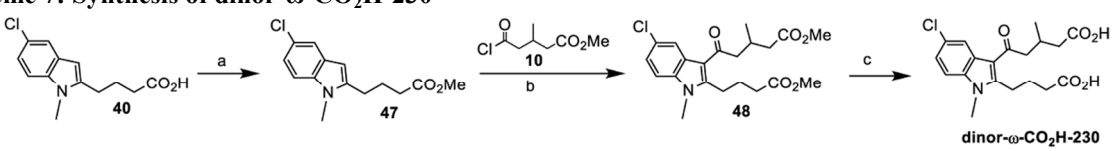

[a]**Reagents and conditions:** (a) KOH, DMSO, CH_3I, 0 °C-rt, 10 h, 78%; (b) Me_2AlCl, CH_2Cl_2, **10**, 0 °C - rt, 30 min, 41%; (c) LiOH, THF, H_2O.

acyl side chain). The identity of the ion at m/z 306 was confirmed by its MS^3 spectrum (Fig. 10E), which includes ions at m/z 288 (loss of H_2O), 262 (loss of CO_2), 246 (loss of $CH_2C(OH)_2$ from the acyl side chain due to a McLafferty rearrangement), 220 (loss of CH_2=CH-CH_2-CO_2H from the acyl side chain due to another McLafferty rearrangement), and 178 (loss of acyl side chain).

In addition to the above three ω1 and ω2 oxidation products, a pair of less polar metabolites that were not present after incubation of **230** with microsomes were observed in plasma extracts (Fig. 10A). The UV spectra of metabolites ***f*** (t_R, 37.76 min with water/acetonitrile) and ***g*** (t_R, 38.60 min with water/acetonitrile) were virtually identical to one another and similar to that of unmetabolized **230** except that the absorbance maximum above 300 nm underwent a bathochromic shift from about 303 nm (**230**) to about 311 nm (***f*** and ***g***) (Fig. 10C). The absorbance maximum at 251 nm also underwent a slight bathochromic shift of about 1 nm, whereas the maximum at 226 nm underwent a small hypsochromic shift of about 2 nm. Metabolites ***f*** and ***g*** were not resolved with a water methanol gradient and had a t_R of 30.2 min (Fig. 10B). Analysis by LC-MS revealed that metabolites ***f*** (m/z 392.1666) and ***g*** (m/z 392.1669) have identical $[M-H]^-$ ions, within 8 ppm of the theoretical value of 392.1634 expected for a monohydroxy metabolite of **230**. However, the MS^2 spectra of ***f*** and ***g***, which were virtually identical to one another, were quite different from those of ω-OH-**230** and ω2-OH-**230**, and were dominated by a single major ion at m/z 292, corresponding to loss of the hydroxyalkyl side chain, along with a much less intense ion at m/z 374 (loss of H_2O) (Fig. 10F). The MS^3 fragmentation pattern of the base peak (m/z 292) in the MS^2 spectrum of ***f*** revealed a pattern similar to that of the ω1- and ω2-hydroxy metabolites, dominated by fragmentation of the

carboxylic acid side chain, with major ions at m/z 274 (loss of H_2O), 248 (loss of CO_2), and 206 (loss of CH_2=CH-CH_2-CO_2H due to a McLafferty rearrangement) (Fig. 10G). This spectrum is virtually identical to the MS^2 fragmentation pattern (Fig. 10H) of the authentic standard ***51*** lacking the hexyl side chain, synthesized as shown in Scheme 8. The facile loss of the hydroxyalkyl side chain as well as the perturbation of the UV spectrum dominated by the indole moiety suggest that the hydroxyl groups of ***f*** and ***g*** are close to the indole, perhaps in the ω6 position of the hexyl side chain (Fig. 10F). Since this would add a second chiral center to the molecule, ***f*** and ***g*** could be diastereomers, which could be separated by RP-HPLC. However, confirmation of these structural assignments would require the availability of the authentic standards.

Scheme 8: Synthesis of 51[a]

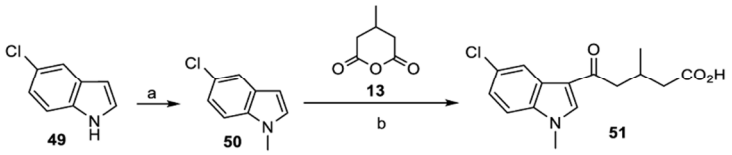

[a]**Reagents and conditions**: (a) NaH, CH_3I, DMF, 0 °C - rt, 18 h, 94%; (b) Me_2AlCl, CH_2Cl_2, **13**, 0 °C - rt, 4 h, 81%.

Antagonist potencies of synthetic 230 metabolites

To determine the effects of oxidative metabolism of **230** on antagonist activity we examined the effects of synthetic metabolites on 5-oxo-ETE-induced calcium mobilization in human neutrophils (Fig. 11). Oxidation of **230** dramatically reduced antagonist potency. Of the compounds tested, ω1-hydroxy-**230** was the most potent, with an IC_{50} value of 270 ± 20 nM, 14 times higher than that of **230** (19 ± 5 nM in this series of experiments). The ω2-oxidized metabolites ω2-hydroxy-**230** and ω2-oxo-**230** were less potent, with IC_{50} values of 1.4 ± 0.3 and 1.6 ± 0.4 μM, respectively. ω-Carboxy-**230** was even less potent, with an IC_{50} of 25 ± 13 μM.

Interestingly, dinor-ω-carboxy-**230** had an IC_{50} (1.3 ± 0.3 μM) similar to the above ω2-oxidized metabolites.

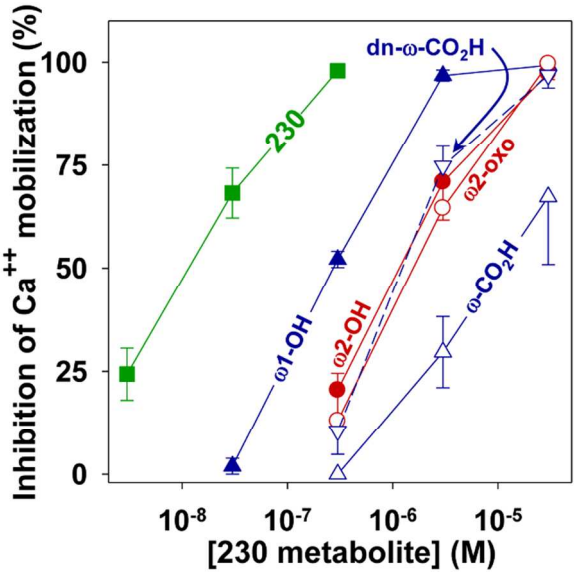

Figure 11. Effects of **230** metabolites on 5-oxo-ETE-induced calcium mobilization in human neutrophils. Calcium mobilization was measured in neutrophils stimulated with 10 nM 5-oxo-ETE 2 min after the addition of either **230** or one of its synthetic metabolites. All compounds are racemic mixtures. Symbols: **230** (■), ω1-hydroxy-**230** (▲), ω2-hydroxy-**230** (●), ω2-oxo-**230** (○), ω-carboxy-**230** (Δ), and dinor-ω-carboxy-**230** (∇). Values are means ± SE of data from between 4 and 5 independent experiments.

DISCUSSION

5-Oxo-ETE is a potent activator of human eosinophils and may be an important mediator in eosinophilic diseases such as asthma. [1] Our previous *in vitro* studies on 5-oxo-ETE antagonists led to the identification of the indole **230** as a potent and selective antagonist of the human OXE receptor. Because there is no ortholog of this receptor in rodents we could not investigate its *in vivo* effects in rat or mouse models of asthma. We recently examined the possibility of using a feline model of asthma for this purpose but found that although 5-oxo-ETE is a highly potent chemoattractant for eosinophils in this species, the OXE receptor antagonists we developed against the human OXE receptor were only weak antagonists of the feline receptor. We therefore

decided to evaluate the cynomolgus monkey as a potential animal model to investigate the effects of our OXE receptor antagonists.

We found that monkey leukocytes synthesize substantial amounts of 5-oxo-ETE directly from 5-HETE as well as from the 5-HETE precursor AA and, as in the case with human granulocytes,[10] this process in enhanced by the NADPH oxidase activator PMA. 12-HETE and 12-HHT were also detected in incubations with AA, presumably because our leukocyte preparations contained platelets bound to monocytes.[11] The results of these experiments indicate that the synthesis of 5-oxo-ETE is regulated similarly in monkey and human leukocytes.

Monkey granulocytes are also very responsive to 5-oxo-ETE. Using flow cytometry and anti-CD49d-labeled leukocytes we were able to identify distinct populations of eosinophils and neutrophils. 5-Oxo-ETE and LTB_4 strongly stimulate actin polymerization in both cell types, with LTB_4 being more potent in the case of neutrophils, as is the case in humans.[12] In contrast, PGD_2 stimulated actin polymerization only in eosinophils, consistent with the lack of the DP_2 receptor in human neutrophils and validating the identity of these two cell populations in our flow cytometry assay.

Both 5-oxo-ETE and LTB_4 are potent chemoattractants for monkey leukocytes. Although LTB_4 is more potent than 5-oxo-ETE in inducing leukocyte migration, the maximal response to 5-oxo-ETE is substantially greater. This was not due to high eosinophil numbers in our leukocyte preparations, which consisted of about 39% neutrophils and only 1% eosinophils. The low eosinophil numbers in these preparations is consistent with the negligible chemotactic response

of these cells to PGD_2. The very high maximal response of monkey leukocytes to 5-oxo-ETE is rather surprizing in view of similar efficacy of 5-oxo-ETE and LTB_4 in inducing human neutrophil migration.[13] It is not clear whether this is because of a difference between species or to the fact that we used unfractionated leukocytes in these experiments rather than purified neutrophils.

Once we established that monkey leukocytes are capable of synthesizing and responding to 5-oxo-ETE we wanted to determine whether the antagonist potency of **230** in this species is similar to that in humans. The potencies of **230** in blocking the stimulatory effects of 5-oxo-ETE on both actin polymerization and leukocyte migration in monkeys were found to be virtually identical to those that we previously reported for humans.[5]

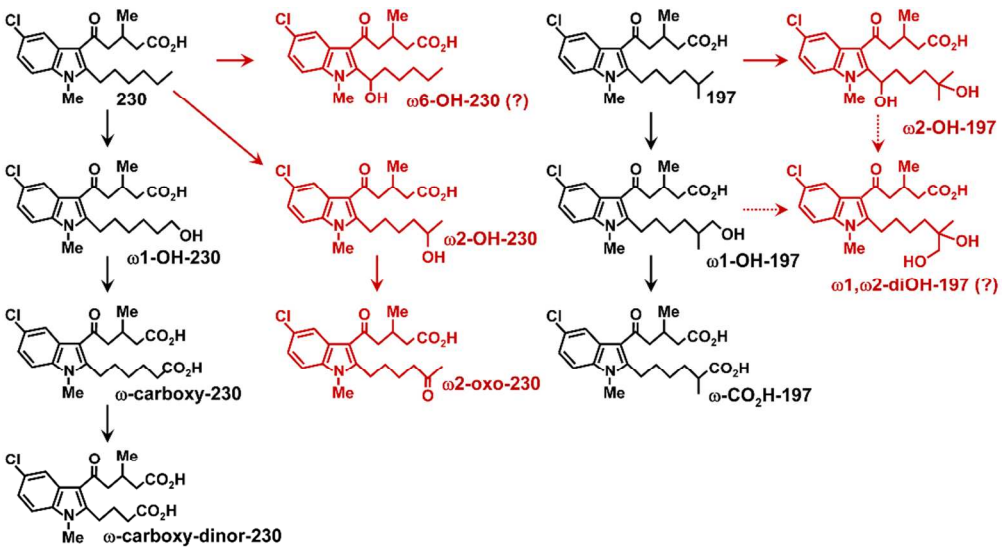

Figure 12. Metabolism of **230** and **197** in monkeys. Major pathways are shown in red.

To investigate the metabolic stability of **230** and to identify its major cytochrome P450-derived metabolites we examined its metabolism by monkey liver microsomes in the presence of NADPH. In contrast to prior experiments with rat liver microsomes, which revealed only modest

metabolism of **230**,[5] we found that **230** is almost completely converted by monkey liver microsomes to two polar metabolites, which were identified as ω2-hydroxy-**230** and ω2-oxo-**230** (Fig. 12) by comparing their chromatographic properties using two mobile phases with different selectivities and their UV and mass spectra with those of authentic standards prepared by total chemical synthesis. We originally anticipated that substantial amounts of ω1-oxidation products would also be formed, since medium- and long- chain fatty acids,[14, 15] prostaglandins,[16] and leukotriene B_4[17] are all converted to significant amounts of both ω1- and ω2- oxidation products by hepatic cytochrome P450 enzymes. However, we detected only small amounts of ω1-hydroxy-**230**, ω-carboxy-**230**, and ω-carboxy-dinor-**230**.

We attempted to reduce the degree of ω-oxidation by adding a branched methyl group at the end of the hexyl side chain, which we hoped would diminish access to the active site of the enzyme due to steric hindrance. We prepared two such compounds with methyl groups in either the ω2-position (**197**) or the ω3-position (**225**) and examined the metabolism of the more potent of these, **197**, which had an IC_{50} virtually identical to that of **230**. However, **197** was metabolized to an extent similar to **230** by monkey liver microsomes, principally to ω2-hydroxy-**197**, with only a small amount of ω1-oxidation to ω1-hydroxy-**197** and ω-carboxy-**197** (Fig. 12). Other substances containing branched chain alkyl groups are also metabolized by ω-oxidation. For example, ω1-oxidation has previously been reported for alkyl-containing compounds with a terminal isopropyl group, such as phylloquinone,[18] tocopherol,[19] and ibuprofen,[20] which are converted by cytochrome P450 isozymes to ω1-hydroxy and ω-carboxy metabolites. Ibuprofen is also metabolized by ω2-hydroxylation[20] and both ω2- and ω3- hydroxylation have been reported

for tocopherols.[21] We speculate that the dihydroxy metabolite of **197** identified by mass spectrometry in the present study is formed by a combination of ω1- and ω2- hydroxylation.

Our next goal was to determine whether significant levels of **230** would appear in blood following oral administration. A pilot experiment in rats revealed that administration of **230** (30 mg/kg) by oral gavage results in plasma levels of over 2 μM, over 50 times higher than its IC_{50} in inhibiting 5-oxo-ETE-induced calcium mobilization in human neutrophils. Consistent with its modest metabolism by rat liver microsomes,[5] no major metabolites were observed in rat plasma. We then conducted more extensive experiments with identical doses of **230** in cynomolgus monkeys that revealed much higher plasma concentrations (~100 μM) that peaked after about 1 hour and then declined to about 1 μM by 24h. The higher blood levels of **230** in monkeys was probably due to a higher rate of absorption from the GI tract rather than to a lower rate of metabolism, as substantial levels of plasma metabolites were observed in this species. **197** also appeared rapidly in the blood, but at lower concentrations than **230**. Interestingly, the plasma levels of the active S-enantiomers of both **230** and **197** were lower than those of the inactive R-enantiomers. In the case of **230**, there was a delay in the selective depletion of the S-enantiomer, as the ratio of S to R enantiomers was about 1:1 for the first hour, and then declined substantially between 2 and 8 h. This suggests that this difference between the two enantiomers was due to selective metabolism of ***S*-230** rather than to selective uptake of the R-enantiomer from the GI tract. On the other hand, the ratio of the S:R enantiomers of **197** was markedly diminished at the earliest time point (30 min), raising the possibility that there might be enantiomeric selectivity at the levels of both absorption and metabolism for this compound. These results suggest that it would be preferable to use pure S-enantiomers for future studies, which will be facilitated by a novel synthetic procedure that we reported very recently.[22]

The profile of plasma metabolites of **230** was more extensive than that which we observed with monkey liver microsomes. As with microsomes, the ω2-oxidation products ω2-hydroxy-**230** and ω2-oxo-**230** were major *in vivo* metabolites, along with much smaller amounts of ω1-oxidation products (mainly ω-carboxy-**230**). However, two major metabolites of intermediate polarity were also detected in plasma. These products, which could be separated from one another by HPLC using an acetonitrile gradient, but not with a methanol gradient, have identical UV and mass spectra, suggesting that they could be stereoisomers. Although the $[M-H]^-$ ions for these isomers indicated the presence of a hydroxyl group, their MS^2 spectra differed markedly from those of the ω1-OH and ω2-OH metabolites discussed above, which are virtually identical to one another. The very intense ion at m/z 292 in these MS^2 spectra would be consistent with a hydroxyl group in the ω6 position, on the carbon adjacent to the indole, although this would need to be confirmed by chemical synthesis. This would be similar to benzylic hydroxylation, a well-known cytochrome P450-catalyzed reaction.[23, 24] Furthermore, a human cytochrome P450 isoform (CYP4Z1) has been reported to hydroxylate both laurate and palmitate in the ω6-position as well as the ω5, ω4, and ω3 positions.[25] Similarly, AA can be hydroxylated in the kidney to give 16- (i.e. ω5), 17-, 18-, 19-, and 20- hydroxy metabolites.[26] We do not know the site of this putative ω6-hydroxylation reaction of **230** in the monkey, but it is likely to be catalyzed by a cytochrome P450 isozyme at a location other than the liver, such as the kidney or the intestines, as we did not observe these products in incubations with liver microsomes.

The pharmacokinetic profile of **230** in monkeys was quite different from what we initially observed in our pilot experiment in rats. In rats, **230** reached a maximal concentration of 2.2 μM by 1 h and remained at that level up to 4 h, before declining to 0.7 μM by 6 h. In monkeys the

concentration of **230** peaked at over 100 μM after only 30 min and then declined to less than 10% of that level by 4 h. However, in spite of the relatively rapid decline in **230** levels in monkeys, its plasma concentration after 24 h (2.7 μM) was higher than the maximum level reached in rats. As we did not detect high levels of **230** metabolites in rats, it is possible that these differences could be due to different rates of absorption from the gut in the two species.

CONCLUSIONS

In conclusion, we have shown that the cynomolgus monkey should be an excellent animal model to investigate the pathophysiological role of 5-oxo-ETE and the efficacy of OXE receptor antagonists. Monkey granulocytes respond very well to 5-oxo-ETE and its effects are blocked by selective OXE receptor antagonists with potencies virtually identical to those in humans. The indole antagonists **230** and **197** rapidly appear in the blood following oral administration, reaching very high concentrations within one hour, and can be detected for up to at least 24 hours. The major *in vivo* pathway for the metabolism of these antagonists is ω2- and possibly also ω6- hydroxylation. It is possible that improved pharmacokinetic profiles could be achieved by structurally blocking one or both of these hydroxylation sites. Although the scope of experiments that can be performed in monkeys is severely limited by the high cost involved, the similarity of the monkey to humans offers an important advantage, given the absence of the OXE receptor in rodents.

EXPERIMENTAL SECTION

Animals. Male and female cynomolgus monkeys weighing between 2.7 to 3.5 kg, housed at INRS-Institut Armand-Frappier, Laval, Quebec, were used for these studies. All experiments were performed in accordance with the guidelines of the Canadian Council on Animal Care and were approved by the local institutional animal care committee.

Preparation of leukocytes from monkey blood. Leukocytes were prepared from whole blood collected in heparinized tubes from monkeys. Blood was treated with Dextran 500 (Sigma-Aldrich) for 45 min at room temperature, followed by hypotonic lysis of red blood cells. After centrifugation, the leukocytes were suspended in phosphate-buffered saline (PBS: 137 mM NaCl, 2.7 mM KCl, 1.5 mM KH_2PO_4, and 8.1 mM Na_2HPO_4, pH 7.4).

Measurement of 5-oxo-ETE by reversed-phase HPLC (RP-HPLC). Monkey leukocytes (2 x 10^6 cells in 1 mL) were resuspended in PBS supplemented with 1.8 mM Ca^{2+} and 1 mM Mg^{2+} (PBS^+) and incubated for various times with either arachidonic acid (30 μM) or 5S-HETE (4 μM) in the presence or absence of A23187 (5 μM) or PMA (100 nM). Incubations were terminated by the addition of methanol (0.65 mL) and cooling to 0 °C. The concentration of methanol in each sample was adjusted to 30% by addition of water prior to analysis by precolumn extraction/RP-HPLC[27] using a modified Waters 2695 Alliance system (Waters Associates, Milford, MA) and a Novapak C18 column (4 μm particle size; 150 x 3.9 mm) as the stationary phase. For AA metabolites, the mobile phase was a linear gradient between H_2O/MeCN/MeOH (44:24:32) and H_2O/MeCN/MeOH (25:55:20) over 40 min with a flow rate of 1 mL/min. Both solvents contained 0.02% HOAc. Incubations with 5-HETE were analyzed as

described above except that the mobile phase was a gradient over 6 min between 60% and 82% MeCN in H_2O containing a final concentration of 0.02% HOAc, followed by isocratic elution with 82% MeCN for 4 min. The identities of the products were confirmed by examination of their UV spectra.

Measurement of F-actin in monkey eosinophils and neutrophils. Leukocytes were prelabeled by incubation for 30 min on ice with allophycocyanin (APC)-labeled mouse antihuman CD49d (BioLegend) as described previously.[8] After washing by centrifugation the cells were resuspended in PBS containing Ca^{2+} (1.8 mM) and Mg^{2+} (1 mM). Aliquots of the leukocyte suspension (100 µl, 5 x 10^6 cells/mL) were preincubated for 5 min at 25°C with either vehicle (1 µl DMSO) or antagonist followed by the addition of either vehicle (10 µl of PBS containing 1% BSA), 5-oxo-ETE, LTB_4 or PGD_2. After 20 s, the incubations were terminated by the addition of formaldehyde (final concentration, 8.5%), and the samples were kept on ice for 30 min. Cytosolic F-actin was stained by incubation with a mixture of lysophosphatidylcholine (30 µg in 23.8 µl of PBS) and N-(7-nitrobenz-2-oxa-1,3-diazol-4-yl)-phallacidin (40.7 pmol in 6.18 µl methanol; final concentration, 1.36 µM) overnight in the dark at 4°C. F-actin levels were measured by flow cytometry in both neutrophils and eosinophils, which were distinguished from one another on the basis of side scatter and CD49d expression.

Evaluation of leukocyte migration. Leukocyte migration was measured as described previously[3] using 48-well microchemotaxis chambers (Neuro Probe, Cabin John, MD) and Sartorius cellulose nitrate filters (8 µm pore size; 140-mm thickness; Neuro Probe). 5-Oxo ETE and either vehicle or antagonists were added to the bottom well in a volume of 30 µl of PBS

containing 1.8 mM $CaCl_2$, 1 mM $MgCl_2$, 0.05% bovine serum albumin and 0.5% DMSO. Leucocytes (150,000 cells in PBS containing 0.05% BSA) and either vehicle (PBS containing 0.5% DMSO) or antagonists were added in a total volume of 55 µl to each of the top wells. Following incubation for 2 h at 37°C, the filters were fixed with mercuric chloride and stained with hematoxylin and chromotrope 2R.[28] The numbers of cells on the bottom surfaces of the filters were counted in five different fields at a magnification of 400x for each incubation, each of which was performed in triplicate.

Evaluation of antagonist potencies in human neutrophils. The abilities of certain analogs and metabolites of **230** to inhibit 5-oxo-ETE-induced Ca^{++} mobilization in human neutrophils were examined as described previously.[5] Neutrophils prepared by dextran sedimentation and centrifugation over Ficoll-Paque were prelabeled with indo-1 and placed in a cuvette at 37°C. After stabilization of baseline fluorescence, antagonist was added, followed 2 min later by 5-oxo-ETE (10 nM) and, 1 min later, by digitonin (final concentration 0.1%). Fluorescence was measured using a Cary Eclipse spectrofluorometer (Agilent Technologies, Santa Clara, CA) equipped with a temperature-controlled cuvette holder and a magnetic stirrer.

RP-HPLC analysis of 230 and 197 metabolites formed by monkey liver microsomes. Liver microsomes (0.5 mg/mL), prepared from a pool of male cynomolgus monkeys (ThermoFisher Scientific), were incubated with **230** or **197** (100 µM) in PBS (without Ca^{++} or Mg^{++}) in the presence of NADPH (2 mM) for 4 h at 37 °C. Reactions were terminated by the addition of methanol and cooling to 0°C. Prior to analysis the concentration of methanol in each sample was adjusted to 30% by addition of water. The products were analyzed by precolumn extraction/RP-

HPLC using a Waters 2695 Alliance system with a Kinetex C18 column (see figure legends for HPLC conditions).

Analysis of 230 and 197 metabolites by LC/MS/MS

The LC-MS/MS analysis of **230** and **197** metabolites was carried out using a model 1100 HPLC system (Agilent Technologies, Santa Clara, CA) connected to LTQ Velos Orbitrap high resolution mass spectrometer via a heated electrospray ionization source (Thermo Scientific, San Jose, CA). Chromatographic separation was performed using a Phenomenex Kinetex C18 column (2.6 µm particle size; 50 x 2.1 mm) at the flow rate of 0.3 mL/min and a column temperature of 25°C. The mobile phase was a gradient between solvents A (water containing 0.02% HOAc) and B (MeCN contained 0.02% HOAc) as follows: 0 min: 30% B; 1 min: 30% B; 20 min: 65% B; 25 min: 65% B. All analyses were performed using an injection volume of 10 µL and negative electrospray ionization (ESI) mode using the following settings: capillary temperature: 350 ^{o}C; source heater temperature: 300 ^{o}C; sheath gas flow: 30; auxiliary gas flow: 10; capillary voltage: - 3.5 kV. The MS settings were: S lens RF level: 60%; automatic gain control (AGC) target: 1 x 10^6 ions; mass range: m/z 250 to m/z 700; resolution: 100,000. Multiple levels of MS^n analysis with data dependent acquisition (DDA) mode were used for the identification and elucidation of antagonist metabolites. In DDA mode the selection of the precursor ion for MS^2 analysis was based on the chlorine isotope pattern and/or isolation of the top three most intense ions from the full MS scan for fragmentation. MS^2 settings also included dynamic exclusion: 10 s; activation type: collision-induced dissociation (CID); signal threshold: 10,000; normalized collision energy: 35: isolation width: 2 Da; activation time: 30 s. MS^3 used parent and product mass lists to trigger MS^3 for selected ions and was performed with CID as

activation type; minimal signal threshold: 5000; isolation width: 2Da; activation time: 30 s; normalized collision energy: 45.

Evaluation of pharmacokinetics of 230 in rats. 230 (30 mg/kg) was administered to Sprague-Dawley rats (6-8 weeks old). **230** was first dissolved in EtOH at a concentration of 75 mg/mL and the appropriate volume added to 10 volumes of 20 mM $NaHCO_3$. The resulting suspension was vortexed and used immediately after preparation. Approximately 1 mL (depending on the weight of the rat) was administered by oral gavage to each rat. After different times the rats were euthanized in a CO_2 chamber and blood was taken by cardiac puncture using sodium citrate as an anticoagulant. Plasma was prepared by centrifugation at 1700 x *g* for 15 min and MeOH (2 volumes) was added to each sample, which was then stored at -80 ^oC prior to analysis. After thawing, samples were centrifuged and H_2O was added to the supernatant to give a final concentration of 30% MeOH. Each sample was loaded onto a Sep-Pak C18 cartridge (Waters),[29] which was washed with 30% MeOH prior to the elution of indole metabolites with 100% MeOH. The eluate was analyzed by precolumn extraction/RP-HPLC[27] using the Waters Alliance system described above with a Novapak column (4 μm particle size; 150 x 3.9 mm). The mobile phase was a gradient between 70 and 100% MeOH containing 0.02% HOAc over 15 min at a flow rate of 1 mL/min and a temperature of 30 ^oC. **197**, added prior to solid-phase extraction, was used as an internal standard.

Evaluation of pharmacokinetics of 230 and 197 in monkeys. 230 and **197** (racemic mixtures in both cases) were administered at a dose of 30 mg/kg. Antagonists were dissolved in EtOH at a concentration of 75 mg/mL and the appropriate volume was then added to 10 volumes of 20 mM

$NaHCO_3$. After vortexing, the resulting suspension (4.4 mL/kg) was administered to monkeys by oral gavage. Blood samples (1 mL) were collected in heparinized tubes and plasma was obtained after centrifugation. After solid-phase extraction using C18 Sep-Paks as described above, samples were analyzed by precolumn extraction/RP-HPLC using a Waters Alliance system. The stationary phase for the pharmacokinetic studies was a Waters Novapak C18 column. The mobile phase was a gradient between 70 and 100% MeOH in H_2O (both containing 0.02% HOAc) over 15 min at a flow rate of 1 mL/min and a temperature of 30 ^oC. **197** was used as an internal standard for measurement of **230** in plasma and **230** was used as an internal standard for measurement of **197**. For experiments designed to identify plasma metabolites of **230** by comparison of their chromatographic properties and UV spectra with those of authentic standards, shallower gradients over longer times were employed (see legend to Fig. 10 for further details).

Statistical analysis. Values are presented as means ± standard error. The statistical significance of differences was determined by 1-way ANOVA using the Student-Newman-Keuls method as a multiple comparison procedure. The value of ‘‘n’’ refers to the number of independent experiments performed on leukocytes or samples from different animals.

Chemical syntheses. All reactions were carried out under an atmosphere of argon using dry solvents. All compounds were analyzed by TLC, NMR and HRMS. ^1H NMR and ^{13}C NMR spectra were recorded at rt on a BRUKER AMX 400 MHz spectrometer in $CDCl_3$, DMSO-d_6 and CD_3OCD_3, using TMS as an internal standard. HRMS were recorded on an AccuTOF mass spectrometer by positive ion ESI mode with DART as an ion source. Prior to biological assay,

the purity of all final compounds was determined to be >95% by a combination of HPLC, NMR and HRMS.

Synthesis of ω-CO_2H-230

*Ethyl 5-chloro-1-methyl-1H-indole-2-carboxylate (**2**).* To a stirred solution of **1** (5.0 g, 25.562 mmol) in DMF (70 mL) was added NaH (3.6 g, 90.009 mmol, 60% dispersion in mineral oil) slowly at 0 °C over a period of 20 min. After 45 min, CH_3I (4.6 mL, 73.890 mmol) was added dropwise at 0 °C. The reaction mixture was stirred at rt for 18 h. The reaction was quenched with the addition of saturated NH_4Cl solution (300 mL) at 0 °C. The organic layer was extracted with EtOAc (3 x 150 mL), washed with brine (2 x 100 mL), dried over Na_2SO_4, and the solvents were removed *in vacuo* to obtain the crude **2**, which was dissolved in hexane and benzene. The removal of the solvents under reduced pressure afforded **2** as a yellow solid (5.7 g, quantitative), which was used without any further purification. HRMS (ESI) *m/z* calcd for $[C_{11}H_{10}ClNO_2 + H]^+$, 224.0478; found 224.0655. ^{1}H NMR (400 MHz, $CDCl_3$): δ 7.63 (s, 1H), 7.30 – 7.29 (m, 2H), 7.20 (s, 1H), 4.05 (s, 3H), 3.91 (s, 3H). ^{13}C NMR ($CDCl_3$): δ 162.3, 137.9, 128.8, 126.6, 126.2, 126.0, 125.6, 120.0, 111.2, 51.5, 32.2.

*(5-Chloro-1-methyl-1H-indol-2-yl)methanol (**3**).* To a stirred solution of **2** (5.7 g, 25.485 mmol) in THF (70 mL) was added $LiAlH_4$ (3.89 g, 102.503 mmol) slowly at 0 °C over a period of 20 min, and the mixture was stirred for 15 min at 0 °C followed by 12 h at rt. 10% v/v H_2SO_4 solution in H_2O (50 mL) was added slowly at 0 °C followed by EtOAc (75 mL). The two layers were separated, and the organic layer was extracted with EtOAc (4 x 75 mL). The combined organic extracts were washed with brine (100 mL), dried over Na_2SO_4, and the solvents were evaporated under reduced pressure to afford **3** as a yellow viscous oil (4.3 g, 86%), which was

used without any further purification. HRMS (ESI) *m/z* calcd for $[C_{10}H_{10}ClNO + H]^+$, 196.0529; found 196.0595. ^{1}H NMR (400 MHz, $CDCl_3$): δ 7.54 (s, 1H), 7.24 – 7.21 (m, 1H), 7.19 – 7.14 (m, 1H), 6.40 (s, 1H), 4.79 (s, 2H), 3.80 (s, 3H). ^{13}C NMR ($CDCl_3$): δ 140.2, 136.9, 128.4, 125.5, 122.6, 120.5, 110.5, 101.3, 57.8, 30.4.

*5-Chloro-1-methyl-1H-indole-2-carbaldehyde (**4**).* To a stirred solution of **3** (4.3 g, 21.978 mmol) in CH_2Cl_2 (50 mL) was added activated MnO_2 (9.49 g, 109.16 mmol) in single portion and the reaction mixture was stirred at rt for 16 h. The mixture was filtered through Celite 545 and silica. The residue was washed thoroughly with CH_2Cl_2. The solvents were evaporated *in vacuo* from the combined filtrate to obtain the crude product, which was purified using flash column chromatography (15% EtOAc/hexane) to afford **4** as yellow solid (3.578 g, 84%). HRMS (ESI) *m/z* calcd for $[C_{10}H_8ClNO + H]^+$, 194.0367; found 194.0255. ^{1}H NMR (400 MHz, $CDCl_3$): δ 9.89 (s, 1H), 7.70 (s, 1H), 7.36 – 7.32 (m, 2H), 7.18 (s, 1H), 4.08 (s, 3H). ^{13}C NMR ($CDCl_3$): δ 182.9, 139.0, 136.4, 127.3, 127.0, 126.6, 122.3, 116.3, 111.6, 31.7.

*(E)-6-(5-chloro-1-methyl-1H-indol-2-yl)hex-5-enoic acid (**6**).* To a stirred suspension of the Wittig salt **5** (3.75 g, 8.459 mmol) in THF (15 mL) was added *t*BuOK (16.9 mL, 1.0 M solution in THF) dropwise at –78 °C. The reaction was allowed to warm to rt and stirred for 40 min. **4** (500 mg, 2.582 mmol) in THF (10 mL) was added dropwise at –78 °C, and the reaction mixture was stirred at rt for 6 h. Saturated NH_4Cl solution (25 mL) was added, and the organic layer was extracted with Et_2O (4 x 30 mL). The combined organic layers were washed with brine (2 x 20 mL). The organic layer was back-extracted from the aqueous layer with Et_2O (2 x 20 mL). The organic layers were combined, dried over Na_2SO_4, and the solvents were evaporated to get the crude product, which was purified using silica gel column chromatography (100% CH_2Cl_2) to

obtain **6** as a light brown solid (503 mg, 70%). HRMS (ESI) *m/z* calcd for $[C_{15}H_{16}ClNO_2 + H]^+$, 278.0948; found 278.0795. ^{1}H NMR (400 MHz, $CDCl_3$): δ 7.49 (d, *J* = 1.8 Hz, 1H), 7.18 – 7.13 (m, 2H), 7.09 (dd, *J* = 8.7 Hz, 1.9 Hz, 1H), 6.50 (s, 1H), 6.26 (dt, *J* = 15.7 Hz, 7.0 Hz, 1H), 3.68 (s, 3 H), 2.41 – 2.30 (m, 4H), 1.87 – 1.80 (m, 2H). ^{13}C NMR ($CDCl_3$): δ 179.4, 139.6, 136.0, 133.6, 128.8, 125.3, 121.4, 119.6, 119.4, 110.0, 97.6, 33.3, 32.7, 30.0, 24.0.

6-(5-Chloro-1-methyl-1H-indol-2-yl)hexanoic acid (7). To a stirred solution of **6** (500 mg, 1.8 mmol) in EtOH (8 mL) was added palladium, 10 wt. % on activated carbon (50 mg). The solution was degassed, and H_2 was purged in the reaction mixture via a balloon. The reaction mixture was stirred at rt under H_2 for 3 h. The mixture was diluted with CH_2Cl_2, and filtered through Celite 545. The solvents were evaporated under reduced pressure to obtain **7** as a yellow solid (460 mg, 91%), which was used further without any purification. HRMS (ESI) *m/z* calcd for $[C_{15}H_{18}ClNO_2 + H]^+$, 280.1104; found 280.1403.^{1}H NMR (400 MHz, $CDCl_3$**)**: δ 7.48 (d, *J* = 1.8 Hz, 1H), 7.16 (d, *J* = 8.6 Hz, 1H), 7.09 (dd, *J* = 8.6 Hz, 1.8 Hz, 1H), 6.18 (s, 1H), 3.64 (s, 3H), 2.73 (t, *J* = 7.6 Hz, 2H), 2.39 (t, *J* = 7.4 Hz, 2H), 1.68 – 1.79 (m, 4H), 1.45 – 1.53 (m, 2H). ^{13}C NMR ($CDCl_3$): δ 178.9, 142.4, 135.8, 128.8, 124.9, 120.7, 119.1, 109.7, 98.5, 33.8, 29.6, 28.7, 28.1, 26.6, 24.4.

*Methyl 6-(5-chloro-1-methyl-1H-indol-2-yl)hexanoate (**9**).* To a stirred solution of **7** (275 mg, 0.983 mmol) in Et_2O (5 mL) was added CH_2N_2 (**8**) (freshly prepared from methylnitronitrosoguanidine and KOH) in Et_2O dropwise. The reaction mixture was stirred at rt for 2 min. The solvents were evaporated under reduced pressure to obtain the ester **9** in quantitative yield. HRMS (ESI) *m/z* calcd for $[C_{16}H_{20}ClNO_2 + H]^+$, 294.1261; found 294.1577. ^{1}H NMR (400 MHz, $CDCl_3$): δ 7.48 (s, 1H), 7.16 – 7.07 (m, 2H), 6.18 (s, 1H), 3.67 (s, 3H), 3.63

(s, 3H), 2.72 (t, *J* = 7.0 Hz, 2H), 2.34 (t, *J* = 7.2 Hz, 2H), 1.77 – 1.66 (m, 4H), 1.51 – 1.42 (m, 2H). ^{13}C NMR ($CDCl_3$): δ 174.1, 142.5, 135.8, 128.8, 124.9, 120.7, 119.1, 109.7, 98.5, 51.5, 33.9, 29.6, 22.9, 28.1, 26.7, 24.7.

*6-(3-(4-Carboxy-3-methylbutanoyl)-5-chloro-1-methyl-1H-indol-2-yl)hexanoic acid (**ω-CO$_2$H-230**).* To a stirred solution of **8** (26 mg, 0.088 mmol) in CH_2Cl_2 (2 mL) was added Me_2AlCl (0.5 mL, 1.0 M solution in hexanes) at 0 °C. The reaction mixture was allowed to warm to rt, and after 20 min methyl 5-chloro-3-methyl-5-oxopentanoate (**10**) (80 mg, 0.448) in CH_2Cl_2 (5 mL) was added followed by CH_3NO_2 (1 mL). The reaction mixture was stirred at rt for 3 h. Saturated NH_4Cl solution (4 mL) was added. The two layers were separated, and the organic layer was extracted with EtOAc (4 x 10 mL), the combined organic layers were washed with brine (5 mL), dried over Na_2SO_4, and then the solvents were evaporated under reduced pressure to obtain the crude bis-ester **11**, which was dissolved in THF (3 mL) and then added LiOH (30 mg, 1.253 mmol) in H_2O (1 mL). The reaction mixture was stirred at rt for 36 h. After removal of about 70% of the solvent, 1 M HCl (2 mL) was added at 0 °C dropwise. After 20 min, the brown precipitate was filtered, washed with cold water and hexane, dried under vacuum, and then purified using flash column chromatography (10% MeOH/$CHCl_3$) to obtain **ω-CO$_2$H-230** (18 mg, 50% over two steps). HRMS (ESI) *m/z* calcd for $[C_{21}H_{26}ClNO_5 + H]^+$, 408.1578; found 408.1541.^{1}H NMR (400 MHz, $CDCl_3$): δ 7.91 (s, 1H), 7.27 – 7.22 (m, 2H), 3.71 (s, 3H), 3.23 – 3.12 (m, 2H), 3.05 – 2.94 (m, 2H), 2.76 – 2.74 (m, 1H), 2.54 – 2.49 (m, 1H), 2.36 – 2.38 (m, 3H), 1.71 – 1.52 (m, 6H), 1.15 (d, *J* = 5.8 Hz, 3H).^{13}C NMR ($CDCl_3$): δ 195.2, 179.2, 178.2, 150.6, 135.2, 128.0, 127.0, 122.4, 120.9, 113.2, 110.7, 49.2, 41.2, 33.8, 29.7, 28.9, 28.6, 26.4, 26.1, 24.3, 20.8.

Synthesis of ω1-OH-230

*6-(5-chloro-1-methyl-1H-indol-2-yl)hexan-1-ol (**12**).* To a stirred solution of **7** (100 mg, 0.3575 mmol) in THF (5 mL) was added $LiAlH_4$ (100 mg, 2.635 mmol) at 0 °C over a period of 10 min. The reaction mixture was then stirred at rt for 14 h. Aqueous NH_4Cl solution (5 mL) was added slowly at 0 °C. The organic layer was extracted with EtOAc (3 x 10 mL), the combined organic extracts were washed with brine (10 mL), dried over Na_2SO_4, and the solvent evaporated under reduced pressure to obtain the crude product, which was chromatographed over silica (40% EtOAc/hexane) to afford **12** as a yellow solid (78 mg, 82%). HRMS (ESI) *m/z* calcd for $[C_{15}H_{20}ClNO + H]^+$, 266.1312; found 266.1302.^{1}H NMR (400 MHz, $CDCl_3$): δ 7.45 (s, 1H), 7.10 (d, *J* = 8.6 Hz, 1H), 7.05 (dd, *J* = 8.6 Hz, *J* = 1.24 Hz, 1H), 6.15 (s, 1H), 3.61 (t, *J* = 6.5, 2H), 3.57 (s, 3H), 2.67 (t, *J* = 7.6, 2H), 1.73 – 1.66 (m, 2H), 1.60 – 1.53 (m, 2H), 1.47 – 1.39 (m, 4H). ^{13}C NMR ($CDCl_3$): δ 142.9, 135.8, 128.9, 124.8, 120.5, 119.1, 109.7, 98.4, 62.9, 32.7, 29.6, 29.2, 28.4, 26.8, 25.6.

*5-(5-chloro-2-(6-hydroxyhexyl)-1-methyl-1H-indol-3-yl)-3-methyl-5-oxopentanoic acid **(ω1-OH-230**).* To a stirred solution of **12** (73 mg, 0.275 mmol) in CH_2Cl_2 (2 mL) was added Me_2AlCl (1.5 mL, 1.0 M solution in hexanes) dropwise at 0 °C. After 40 min of stirring at rt, 3-methylglutaric anhydride **13** (57 mg, 0.445mmol) was added in a single portion followed by CH_3NO_2 (1 mL). The reaction mixture was stirred at rt for 6 h. Saturated NH_4Cl solution (5 mL) was added, and the organic layer was extracted with $CHCl_3$ (3 x 5 mL), the combined organic extracts were washed with brine (10 mL). The organic layer was back-extracted from the aqueous layer using EtOAc (3 x 10 mL). The organic extracts were combined, dried over Na_2SO_4, and the solvents were evaporated to obtain the crude product, which was purified using silica gel column chromatography (2-3% MeOH/CH_2Cl_2) to obtain the desired product **ω1-OH-230** as a yellow

solid (46 mg, 43%). HRMS (ESI) *m/z* calcd for $[C_{21}H_{28}ClNO_4 + H]^+$, 394.1785; found 394.1904. ^{1}H NMR (400 MHz, $CDCl_3$ + D_2O): δ 7.91 (s, 1H), 7.27 – 7.17 (m, 2H), 3.71 – 3.63 (m, 5H), 3.20 – 3.08 (m, 2H), 3.04 – 2.88 (m, 2H), 2.76 – 2.67 (m, 1H), 2.51 (dd, *J* = 14.9 Hz, 5.7 Hz, 1H), 2.33 (dd, *J* = 15.1Hz, 7.0 Hz, 1H), 1.64 – 1.50 (m, 8H), 1.12 (d, *J* = 6.6 Hz, 3H). ^{13}C NMR ($CDCl_3$): δ 195.4, 177.1, 150.8, 135.1, 128.0, 127.0, 122.3, 120.5, 113.1, 110.7, 62.6, 49.0, 41.1, 32.2, 29.7, 29.2, 28.9, 26.5, 26.1, 25.2, 20.5.

Synthesis of ω2-OH-230

*5-Iodopentan-2-ol (**15**).* A regioselective cleavage of 2-methyltetrahydrofuran (**14**) to obtain 5-iodopentan-2-ol (**15**) was carried using a modified procedure reported previously.[30] CH_2Cl_2 (60 mL) was added to $Et4N^+I^-$ (14.735 g, 57.299 mmol) in a 250 mL round bottom flask equipped with a stirring bar. To this suspension was added **14** (4.9 mL, 48.582 mmol) followed by $BF_3.Et_2O$ (7.2 mL) slowly. After stirring the reaction mixture at rt for 16 h, saturated $NaHCO_3$ solution (60 mL) was added and the two layers were separated. The aqueous layer was extracted with CH_2Cl_2 (3 x 50 mL). The combined organic extracts were washed with water (50 mL) and brine (100 mL), and dried over Na_2SO_4. The solvents were evaporated under reduced pressure to obtain the crude product, which was purified using silica gel column chromatography (10% Et_2O/EtOAc) to obtain **15** as colorless oil (4.958 g, 48%). ^{1}H NMR (400 MHz, $CDCl_3$): δ 3.89 – 3.83 (m, 1H), 3.23 (t, *J* = 6.9 Hz, 2H), 2.10 (br s, 1H), 2.04 – 1.83 (m, 2H), 1.63 – 1.50 (m, 2H), 1.23 (d, *J* = 6.2 Hz, 3H). ^{13}C NMR ($CDCl_3$): δ 67.4, 39.8, 29.8, 23.7, 6.9.

*2-((5-Iodopentan-2-yl)oxy)tetrahydro-2H-pyran (**16**).* To a stirred solution of **15** (2.1 g, 9.811 mmol) in THF (30 mL) was added PPTS (247 mg, 0.9811 mmol) at once followed by DHP (1.34 mL, 14,717 mmol) dropwise. The reaction mixture was stirred at rt for 3.5 h. The reaction was

quenched by adding saturated $NaHCO_3$ solution (40 mL) and the organic layer was extracted with Et_2O (3 x 35 mL). The combined organic extracts were washed with brine (50 mL) and dried over Na_2SO_4. The solvents were evaporated under reduced pressure to obtain the crude product, which was purified using silica gel column chromatography (3% EtOAc/hexane) to afford **16** as colorless oil (2.634 g, 90%). ^{1}H NMR (400 MHz, $CDCl_3$): δ 4.67 (t, *J* = 3.8 Hz, 1H), 4.63 (t, *J* = 4.4 Hz, 1H), 3.94 – 3.71 (m, 4H), 3.52 – 3.48 (m, 2H), 3.28 – 3.20 (m, 4H), 2.17 – 1.54 (m, 20H), 1.24 (d, *J* = 6.3 Hz, 3H), 1.24 (d, *J* = 6.3 Hz, 3H). 1.13 (d, *J* = 6.1 Hz, 3H). ^{13}C NMR ($CDCl_3$): δ 98.8, 95.9, 73.1, 70.0, 62.9, 62.8, 38.2, 37.3, 31.2, 30.3, 29.9, 29.5, 25.52, 25.48, 21.6, 20.0, 19.9, 7.4, 7.1.

*(Z)-6-(5-chloro-1-methyl-1H-indol-2-yl)hex-5-en-2-ol (**18**).* To a stirring solution of **16** (2.6 g, 8.720 mmol) in CH_3CN (28 mL) was added PPh_3 (2.29 g, 8.731 mmol) and the reaction mixture was refluxed gently (85 °C) for 47 h. The solvents were evaporated under reduced pressure and the crude product was washed with benzene to afford the crude **17** as white solid (4.398 g). To a stirred suspension of **17** (1.6 g, 2.855 mmol) in THF (7 mL) was added KHMDS (4.2 mL, 1.0 M solution in THF) at –78 °C. The mixture was warmed to rt and stirred for 40 min. The aldehyde (362 mg, 1.869 mmol) in THF (4 mL) was added at –78 °C. The reaction mixture was then stirred at rt for 4 h. Saturated NH_4Cl solution (20 mL) was added slowly. The mixture was diluted with EtOAc. The two layers were separated and the organic layer was extracted with EtOAc (3 x 25 mL). The combined organic extracts were washed with brine (25 mL), dried over Na_2SO_4, and the solvents were evaporated under reduced pressure to obtain the crude product, which was purified using silica gel column chromatography (40% EtOAc/hexane) to yield **18** (285 mg, 58%) as a yellow viscous oil. In this Wittig reaction, a THP group was removed, presumably because of the aqueous NH_4Cl solution work-up.[31] HRMS (ESI) *m/z* calcd for

$[C_{15}H_{18}ClNO + H]^+$, 264.1155; found 264.1149. ^{1}H NMR (400 MHz, $CDCl_3$): δ 7.53 (d, *J* = 1.7 Hz, 1H), 7.18 (d, *J* = 8.7 Hz, 1H), 7.12 (dd, *J* = 8.7 Hz, 1.9 Hz, 1H), 6.45 (s, 1H), 6.39 (d, *J* = 11.6 Hz, 1H), 5.90 (dt, *J* = 11.6 Hz, 7.2 Hz, 1H), 3.88 – 3.84 (m, 1H), 3.66 (s, 3H), 2.55 – 2.47 (m, 2H), 1.69 – 1.59 (m, 2H), 1.21 (d, *J* = 6.2 Hz, 3H). ^{13}C NMR ($CDCl_3$): δ 137.4, 135.9, 135.4, 128.8, 125.2, 121.8, 119.6, 117.9, 110.0, 101.4, 67.7, 38.8, 30.0, 25.8, 23.7.

*6-(5-chloro-1-methyl-1H-indol-2-yl)hexan-2-ol (**19**).* To a stirred solution of **18** (125 mg, 0.474 mmol) was added EtOH (2.5 mL). Palladium, 10 wt. % on activated carbon (13 mg) was added at once, and the reaction flask was sealed and degassed. Then, a H_2 balloon was charged and the reaction mixture was stirred at rt. After 3 h, the mixture was diluted with CH_2Cl_2 and filtered through Celite 545 and silica. The residue was washed with CH_2Cl_2. The combined filtrate was evaporated *in vacuo* to obtain **19** as a yellow viscous oil (126 mg, quantitative). HRMS (ESI) *m/z* calcd for $[C_{15}H_{20}ClNO + H]^+$, 266.1312; found 266.1234. ^{1}H NMR (400 MHz, $CDCl_3$): δ 7.47 (d, *J* = 1.8 Hz, 1H), 7.16 (d, *J* = 8.6 Hz, 1H), 7.08 (dd, *J* = 8.6 Hz, 2.0 Hz, 1H), 6.19 (s, 1H), 3.84 – 3.79 (m, 1H), 3.64 (s, 3H), 2.73 (t, *J* = 7.7 Hz, 2H), 1.78 – 1.68 (m, 2H), 1.59 – 1.42 (m, 4H), 1.21 (d, *J* = 6.2 Hz, 3H). ^{13}C NMR ($CDCl_3$): δ 142.6, 135.8, 128.8, 124.9, 120.7, 119.1, 109.6, 98.5, 68.0, 39.0, 29.6, 28.5, 26.8, 25.6, 23.7.

*5-(5-Chloro-2-(5-hydroxyhexyl)-1-methyl-1H-indol-3-yl)-3-methyl-5-oxopentanoic acid (**ω2-OH-230**).* To a stirred solution of **19** (14 mg, 0.053 mmol) in CH_3NO_2 (0.3 mL) was added Me_2AlCl (0.3 mL. 1.0 M solution on hexanes) at rt. After 30 min, 3-methyl glutaric anhydride (**13**) (10 mg, 0.078 mmol) was added at once, and the reaction mixture was stirred at rt for 3 h. The reaction was quenched with saturated NH_4Cl solution (2 mL). The organic layer was extracted with EtOAc (5 x 5 mL). The combined organic layers were washed with brine (10 mL),

dried over Na_2SO_4, and the solvents were evaporated under reduced pressure to obtain the crude product, which was purified by a silica gel column chromatography (10% MeOH/CH_2Cl_2) to obtain **ω2-OH-230** as a brown viscous oil (17 mg, 82%) containing an inseparable pair of diastereomers. HRMS (ESI) *m/z* calcd for $[C_{21}H_{28}ClNO_4 + H]^+$, 394.1785; found 394.1670.

Synthesis of ω2-oxo-230

*5-(5-Chloro-1-methyl-2-(5-oxohexyl)-1H-indol-3-yl)-3-methyl-5-oxopentanoic acid (**ω2-oxo-230**).* To a stirred solution of **ω2-OH-230** (36 mg, 0.914 mmol) in CH_2Cl_2 (5 mL) was added DMP (53 mg, 0.125 mmol) in a single portion at rt, and the reaction mixture was stirred at rt for 9 h. The mixture was filtered through Celite 545, and the combined filtrates were evaporated under reduced pressure to obtain the crude product that was purified using silica gel column chromatography (1-2% MeOH/CH_2Cl_2) to obtain **ω2-oxo-230** as a yellow viscous oil (23 mg, 64%). HRMS (ESI) *m/z* calcd for $[C_{21}H_{26}ClNO_4 + H]^+$, 392.1629; found 392.1796. ^{1}H NMR (400 MHz, $CDCl_3$): δ 7.87 (s, 1H), 7.25 – 7.21 (m, 2H), 3.72 (s, 3H), 3.24 – 3.15 (m, 2H), 3.06 – 2.95 (m, 2H), 2.76 – 2.70 (m, 1H), 2.55 – 2.51 (m, 3H), 2.38 (dd, *J* = 14.7 Hz, *J* = 6.8 Hz, 1H), 2.15 (s, 3H), 1.77 – 1.59 (m, 4H), 1.16 (d, *J* = 6.7 Hz, 3H). ^{13}C NMR ($CDCl_3$): δ 209.2, 195.5, 173.7, 150.7, 135.2, 128.1, 126.8, 122.4, 120.4, 113.1, 110.8, 77.2, 49.1, 43.1, 30.1, 29.7, 28.3, 26.5, 26.1, 23.7, 20.7.

Synthesis of 197

*(E)-5-chloro-2-(5-methylhex-1-en-1-yl)-1H-indole (**22**, R^1 = H, R^2 = CH_3).* To a stirred suspension of (4-methylpentyl)triphenylphosphonium bromide **21** (9.75 g, 22.4 mmol) in THF (30 mL) was added LiHMDS (19 mL, 1.0 M solution in THF) at –78 °C. The reaction was allowed to warm to rt and stirred for 30 min. 5-chloro-1*H*-indole-2-carbaldehyde **20** (1.6 g, 8.958

mmol) in THF (30 mL) was added at –78 °C dropwise over a period of 10 min. The reaction mixture was warmed to rt and stirred for 2.5 h. Saturated NH_4Cl solution (50 mL) was added, and the organic layer was extracted with EtOAc (3 x 50 mL). The combined organic layers were washed with brine (50 mL). The organic layer was dried over Na_2SO_4, and the solvents were evaporated to get the crude product, which was purified using silica gel column chromatography (15% EtOAc/hexanes) to obtain **22**, R^1 = H, R^2 = CH_3, as orange solid (2.0 g, 90%) with a trans/cis ratio of 98/2.[5] HRMS (ESI) *m/z* calcd for $[C_{15}H_{18}ClN + H]^+$, 248.1206; found 248.1216. ^{1}H NMR (400 MHz, $CDCl_3$): δ 8.06 (s, 1H), 7.47 (d, *J* = 1.8 Hz, 1H), 7.18 – 7.06 (m, 2H), 6.43 – 6.31 (m, 2H), 6.07 (dt, *J* = 16.0 Hz, 7.2Hz, 1H), 2.27 – 2.21 (m, 2H), 1.65 – 1.58 (m, 1H), 1.39 – 1.33 (m, 2H), 0.93 – 0.91 (m, 6H). ^{13}C NMR ($CDCl_3$): δ 136.7, 130.2, 128.7, 128.5, 124.1, 120.9, 118.9, 118.3, 110.0, 99.4, 37.7, 29.5, 26.2, 21.2, 21.1.

*5-chloro-2-(5-methylhexyl)-1H-indole (**23**, R^1 = H, R^2 = CH_3).* To a stirred solution of **22**, R^1 = H, R^2 = CH_3, (1.42 g, 5.731 mmol) in EtOH (23 mL) was added palladium, 10 wt. % on activated carbon (160 mg), and the mixture was stirred under argon for 10 min. The reaction flask was then degassed under vacuum, and H_2 was purged in the reaction mixture via a balloon. The reaction mixture was stirred at rt under H_2 for 5 h. The reaction mixture was then filtered through Celite 545 and the residue was rinsed with CH_2Cl_2. The solvents were removed under reduced pressure to obtain the crude product as a red solid, which was purified using flash column chromatography (15% EtOAc/hexane) to obtain the desired product **23**, R^1 = H, R^2 = CH_3, as a yellow solid (1.30 g, 91%) HRMS (ESI) *m/z* calcd for $[C_{15}H_{20}ClN + H]^+$, 250.1363; found 250.1359. ^{1}H NMR (400 MHz, $CDCl_3$): δ 7.86 (s, 1H), 7.47 (d, *J* = 1.8 Hz, 1H), 7.19 – 7.04 (m, 2H), 6.17 (s, 1H), 2.73 (t, *J* = 7.3 Hz, 2H), 1.70 – 1.67 (m, 2H), 1.57 – 1.52 (m, 1H),

1.42 – 1.34 (m, 2H), 1.24 – 1.21 (m, 2H), 0.89 – 0.86 (m, 6 H). ^{13}C NMR ($CDCl_3$): δ 141.6, 134.1, 130.0, 125.2, 121.1, 119.2, 111.1, 99.3, 38.7, 29.3, 28.3, 27.9, 27.1, 22.6 (2C).

*5-Chloro-1-methyl-2-(5-methylhexyl)-1H-indole (**24**, R^1 = H, R^2 = CH_3).* To a stirred solution of **23**, R^1 = H, R^2 = CH_3, (1.2 g, 4.804 mmol) in DMSO (20 mL) was added KOH (1.35 g, 24 mmol) in one portion at 0 °C, and then allowed to warm to rt. After stirring the reaction mixture for 1 h at rt, CH_3I (1.5 mL, 24 mmol) was added dropwise at 0 °C. The reaction mixture was then stirred at rt for 3 h. Saturated NH_4Cl solution (50 mL) was added and the aqueous layer was extracted with EtOAc (3 x 40 mL). The combined organic layers were washed with brine (50 mL) and dried over Na_2SO_4. The solvents were evaporated using a rotary evaporator to obtain the crude product that was purified by flash column chromatography (3% EtOAc/hexane) to obtain the desired product **24** as a yellow viscous oil (1.2 g, 95%). HRMS (ESI) *m/z* calcd for $[C_{16}H_{22}ClN + H]^+$, 264.1519; found 264.1511. ^{1}H NMR (400 MHz, $CDCl_3$): δ 7.47 (d, *J* = 1.8 Hz, 1H), 7.15 – 7.06 (m, 2H), 6.17 (s, 1H), 3.62 (s, 3H), 2.69 (t, *J* = 7.3 Hz, 2H), 1.68 – 1.67 (m, 2H), 1.57 – 1.51 (m, 1H), 1.49 – 1.42 (m, 2H), 1.25 – 1.23 (m, 2H), 0.89 – 0.88 (m, 6H). ^{13}C NMR ($CDCl_3$): δ 143.0, 135.7, 128.9, 124.8, 120.6, 119.0, 109.6, 98.3, 38.8, 29.5, 28.7, 27.9, 27.2, 26.9, 22.6 (2C).

*5-(5-chloro-1-methyl-2-(5-methylhexyl)-1H-indol-3-yl)-3-methyl-5-oxopentanoic acid (**197**).* To a stirred solution of **24**, R^1 = H, R^2 = CH_3, (200 mg, 0.758 mmol) in CH_2Cl_2 (2 mL) Me_2AlCl (4 mL, 1.0 M solution in hexanes) was added dropwise at rt. After 30 min, 3-methylglutaric anhydride **6** (800 mg, 6.244 mmol) was added in a single portion at rt, and the reaction mixture was stirred at rt for 3 h. Saturated NH_4Cl solution (4 mL) was added, and the organic layer was extracted with EtOAc (3 x 5 mL), the combined organic extracts were washed with brine (20

mL), dried over Na_2SO_4, and the solvents were evaporated to obtain the crude product, which was purified using silica gel column chromatography (100% CH_2Cl_2) to obtain the product as yellow oil (90 mg, 64%). HRMS (ESI) *m/z* calcd for $[C_{22}H_{30}ClNO_3 + H]^+$, 392.1992; found 392.1759. ^{1}H NMR (400 MHz, $CDCl_3$): δ 7.90 (d, *J* = 1.4 Hz, 1H), 7.23 – 7.20 (m, 2H), 3.71 (s, 3H), 3.19 – 3.15 (m, 2H), 3.01 – 2.93 (m, 2H), 2.77 – 2.73 (m, 1H), 2.57 (dd, *J* = 15.3 Hz, 3.5 Hz, 1H), 2.39 – 2.33 (m, 1H), 1.64 – 1.44 (m, 5H), 1.24 – 1.22 (m, 2H), 1.14 (d, *J* = 6.4 Hz, 3H), 0.89 – 0.87 (m, 6H). ^{13}C NMR ($CDCl_3$): δ 195.3, 177.3, 151.1, 135.2, 128.0, 127.0, 122.3, 120.4, 113.1, 110.6, 49.0, 40.9, 38.7, 29.7, 29.4, 28.0, 27.8, 26.5, 26.4, 22.6 (2C), 20.5.

Synthesis of 225

*5-(5-chloro-1-methyl-2-(4-methylhexyl)-1H-indol-3-yl)-3-methyl-5-oxopentanoic acid (***225***)*. **225** was prepared by using the same method as described for **197** (Scheme 3). HRMS (ESI) *m/z* calcd for $[C_{22}H_{30}ClNO_3 + H]^+$, 392.1992; found 392.1759. ^{1}H NMR (400 MHz, $CDCl_3$): δ 7.80 (d, *J* = 1.4 Hz, 1H), 7.15 – 7.12 (m, 2H), 3.62 (s, 3H), 3.11 – 3.00 (m, 2H), 2.96 – 2.84 (m, 2H), 2.69 – 2.59 (m, 1H), 2.47 (dd, *J* = 15.1 Hz, 5.6 Hz, 1H), 2.30 – 2.23 (m, 1H), 1.55 – 1.16 (m, 7H), 1.05 (d, *J* = 6.7 Hz, 3H), 0.78 – 0.75 (m, 6H). ^{13}C NMR ($CDCl_3$): δ 195.4, 176.8, 151.2, 135.2, 128.0, 127.0, 122.3, 120.4, 113.1, 110.7, 49.0, 40.9, 36.7, 34.2, 29.7, 29.4, 26.7, 26.64, 26.57, 20.5, 19.1, 11.4.

Synthesis of ω1-OH-197

Diethyl 2-(3-bromopropyl)-2-methylmalonate (27). A synthesis of the intermediate diethyl 2-(3-bromopropyl)-2-methylmalonate (**27**) was adopted from Chen, Hsiu-Yi *et al.*[32] with modifications. Accordingly, to a stirred solution of **25** (3.12 g, 17.2 mmol) in DMF (30 mL), NaH (0.756 g, 18.9 mmol, 60% dispersion in mineral oil) was added slowly at 0 °C over a period

of 20 min. After 45 min, 1,3-dibromopropane (**26**) (5.29 g, 25.8 mmol) was added dropwise at 0 °C. The reaction mixture was stirred at rt for 2 h. The reaction was quenched with the addition of saturated NH_4Cl solution (40 mL) at 0 °C. The aqueous layer was extracted with Et_2O (3 × 50 mL), which was washed with brine (2 × 30 mL), dried over Na_2SO_4, and the solvents then removed *in vacuo*. The crude product was purified by silica gel column chromatography (5% EtOAc in Hexane) to obtain **27** as a light yellow liquid (3.55 g, 70%). HRMS (ESI) *m/z* calcd for $[C_{11}H_{19}BrO_4 + H]^+$, 295.0539; found 295.0325. ^{1}H NMR (400 MHz, $CDCl_3$): δ 4.13 (q, *J* = 7.2 Hz, 4H), 3.36 (t, *J* = 6.6 Hz, 2H), 2.00– 1.94 (m, 2H), 1.85– 1.76 (m, 2H), 1.39 (s, 3H), 1.22 (t, *J* = 7.1 Hz, 6H); ^{13}C NMR ($CDCl_3$): δ 171.9 (2C), 61.3 (2C), 53.1, 34.3, 33.2, 27.9, 20.0, 14.0 (2C).

*6-Bromo-2-methylhexanoic acid (**28**).* To a stirred solution of **27** (6.50 g, 22.0 mmol) in Ac_2O (10 mL) was added HBr (48%, 10 mL), and the solution was refluxed at 150 °C for 16 h. The reaction mixture was cooled to rt, concentrated at reduced pressure, and diluted with water (10 mL). The organic layer was extracted with EtOAc (3 × 30 mL), washed with brine (2 × 60 mL), dried over Na_2SO_4, and the solvents were removed *in vacuo* to obtain crude **28** as a light yellow liquid (3.11 g, 72%), which was used without any further purification. HRMS (ESI) *m/z* calcd for $[C_6H_{11}BrO_2 + H]^+$, 195.0020; found 194.9811. ^{1}H NMR (400 MHz, $CDCl_3$): δ 3.42 (td, *J* = 6.6, 1.7 Hz, 2H), 2.72 – 2.41 (m, 1H), 1.97 – 1.75 (m, 3H), 1.69 – 1.58 (m, 1H), 1.22 (d, *J* = 7.0 Hz, 3H); ^{13}C NMR ($CDCl_3$): δ 182.1, 38.6, 33.2, 32.0, 30.3, 17.0.

*(5-Carboxyhexyl)triphenylphosphonium bromide (**29**).* To a stirred solution of **28** (0.558 g, 2.88 mmol) in CH_3CN (2 mL) was added PPh_3 (2.26 g, 8.63 mmol) and the reaction mixture was refluxed for 18 h. The solvents were evaporated under reduced pressure and the crude product

purified using silica gel column chromatography (10% MeOH in CH_2Cl_2) to afford **29** as a white solid (0.924 g, 70%). HRMS (ESI) *m/z* calcd for $[C_{24}H_{26}O_2P]^+$, 377.1665; found 377.1220. ^{1}H NMR (400 MHz, $CDCl_3$): δ 7.93 – 7.77 (m, 10H), 7.74 – 7.69 (m, 5H), 4.19 – 3.97 (m, 1H), 3.37 – 3.09 (m, 2H), 2.04 – 1.91 (m, 1H), 1.83 – 1.54 (m, 3H), 1.10 (d, *J* = 6.7 Hz, 3H). ^{13}C NMR ($CDCl_3$): δ 178.3, 135.2 (3C), 133.6 (6C), 130.6 (6C), 118.0 (3C), 38.6, 34.4, 22.5, 20.2, 17.5.

*6-(5-Chloro-1-methyl-1H-indol-2-yl)-2-methylhex-5-enoic acid (**30**).* To a stirred suspension of **29** (0.914 g, 2.00 mmol) in THF (3 mL) was added *t*BuOK (4.0 mL, 1.0 M solution in THF) at –10 °C. The mixture was warmed to rt and stirred for 40 min. The aldehyde **4** (400 mg, 2.07 mmol) in THF (4 mL) was added at –10 °C. The reaction mixture was then stirred at rt for 3 h. Saturated NH_4Cl solution (10 mL) was then added slowly and the mixture was diluted with EtOAc. The two layers were separated and the aqueous layer was extracted with EtOAc (3 × 10 mL). The combined organic extracts were washed with brine (25 mL), dried over Na_2SO_4, and the solvents were evaporated under reduced pressure to obtain the crude product, which was purified using silica gel column chromatography (25% EtOAc/hexane) to yield **30** (0.332 g, 57%). HRMS (ESI) *m/z* calcd for $[C_{16}H_{18}ClNO_2 + H]^+$, 292.1099; found 292.0574. ^{1}H NMR (400 MHz, $CDCl_3$): δ 7.48 (d, *J* = 2.3 Hz, 1H), 7.33 (d, *J* = 9.1Hz, 1H), 7.16 – 7.04 (m, 2H), 6.57 – 6.41 (m, 2H), 6.27 (dt, *J* = 15.0, 7.0 Hz, 1H), 3.69 (s, 3H), 2.58 – 2.45 (m, 2H), 2.33 (q, *J* = 7.5 Hz, 2H), 1.92 (dq, *J* = 14.9 Hz, 7.6 Hz, 1H), 1.65 (dq, *J* = 14.0 Hz, 7.1 Hz, 1H), 1.24 (d, *J* = 6.9 Hz, 3H). ^{13}C NMR ($CDCl_3$): δ 182.0, 139.7, 136.0, 133.8, 128.8, 125.3, 121.4, 119.40, 119.36, 110.0, 97.6, 38.7, 32.8, 31.0, 30.0, 17.0

*6-(5-Chloro-1-methyl-1H-indol-2-yl)-2-methylhexanoic acid (**31**).* To a stirred solution of **30** (281 mg, 0.965 mmol) was added EtOH (2.5 mL). Palladium, 10 wt. % on activated carbon (13

mg) was added at once, and the reaction flask was sealed and degassed. Then, a H_2 balloon was charged and the reaction mixture was stirred at rt. After 3 h, the mixture was diluted with CH_2Cl_2 and filtered through Celite 545 and silica. The residue was washed with EtOAc. The combined filtrate was evaporated *in vacuo* to obtain **31** as a yellow viscous oil (281 mg, quantitative). HRMS (ESI) *m/z* calcd for $[C_{16}H_{20}ClNO_2 + H]^+$, 294.12608; found 294.0087. ^{1}H NMR (400 MHz, $CDCl_3$): δ 7.47 (d, *J* = 2.0 Hz, 1H), 7.15 (d, *J* = 8.6 Hz, 1H), 7.11 – 7.04 (m, 1H), 6.18 (s, 1H), 3.63 (s, 3H), 2.72 (t, *J* = 7.7 Hz, 2H), 2.49 (dt, *J* = 14.5 Hz, 7.2 Hz, 1H), 1.70 – 1.79 (m, 3H), 1.50 (td, *J* = 10.1, 6.3 Hz, 3H), 1.20 (d, *J* = 7.0 Hz, 3H). ^{13}C NMR ($CDCl_3$): δ 182.1, 141.9, 135.3, 128.3, 124.4, 120.2, 118.6, 109.2, 98.0, 38.8, 32.8, 29.1, 27.8, 26.4, 26.2, 16.4.

*6-(5-Chloro-1-methyl-1H-indol-2-yl)-2-methylhexan-1-ol (**32**).* To a stirred solution of **31** (281 mg, 959 mmol) in THF (3 mL) was added $LiAlH_4$ (75 mg, 2.0 mmol) slowly at –20 °C over a period of 5 min, and the mixture was stirred at –20 °C for 15 min and then at rt for a further 4 h. 10% v/v H_2SO_4 solution in H_2O (3 mL) was added slowly at –20 °C followed by EtOAc (5 mL). The two layers were separated, and the aqueous layer was extracted with EtOAc (4 × 5 mL). The combined organic extracts were washed with brine (15 mL), dried over Na_2SO_4, and the solvents were evaporated under reduced pressure to afford the crude product, which was purified using silica gel column chromatography (30% EtOAc/hexane) to afford **32** (180 mg, 67%). HRMS (ESI) *m/z* calcd for $[C_{16}H_{22}ClNO + H]^+$, 280.1463; found 280.1112. ^{1}H NMR (400 MHz, $CDCl_3$): δ 7.48 (d, *J* = 2.0 Hz, 1H), 7.16 (d, *J* = 8.6 Hz, 1H), 7.10 (d, *J* = 2.0 Hz, 1H), 6.18 (d, *J* = 1.0 Hz, 1H), 3.64 (s, 3H), 3.57 – 3.38 (m, 2H), 2.72 (t, *J* = 7.7 Hz, 2H), 1.78 – 1.60 (m, 3H), 1.53 – 1.36 (m, 3H), 1.18 (dt, *J* = 10.9 Hz, 7.3 Hz, 1H), 0.93 (d, *J* = 6.7 Hz, 3H). ^{13}C NMR ($CDCl_3$): δ 142.7, 135.7, 128.8, 124.9, 120.6, 119.1, 109.6, 98.4, 68.3, 35.7, 32.9, 29.6, 28.8, 26.83, 26.80, 16.6.

*1-(6-(5-chloro-3-(5-methoxy-3-methyl-5-oxopentanoyl)-1-methyl-1H-indol-2-yl)-2-methylhexyl) 5-methyl 3-methylpentanedioate (**33**).* To a stirred solution of **32** (52.2 mg, 0.187 mmol) in CH_2Cl_2 (1 mL) was added Me_2AlCl (0.6 mL, 1.0 M solution in hexanes) at 0 °C. The reaction mixture was allowed to warm to rt, and after 20 min methyl 5-chloro-3-methyl-5-oxopentanoate (**10**) (89.3 mg, 0.558 mmol) in CH_2Cl_2 (2 mL) was added. After stirring the reaction mixture at rt for 3 h, saturated NH_4Cl solution (4 mL) was added. The two layers were separated, and the aqueous layer was extracted with EtOAc (4 × 10 mL). The combined organic layers were washed with brine (5 mL), dried over Na_2SO_4, and then the solvents were evaporated under reduced pressure to obtain crude **33**, which was purified using silica gel column chromatography (50% EtOAc/hexane) to afford **33** (73.4 mg, 70%) as a pair of diastereomers. HRMS (ESI) *m/z* calcd for $[C_{30}H_{42}ClNO_7 + H]^+$, 564.2723; found 564.2417.

*5-(5-Chloro-2-(6-hydroxy-5-methylhexyl)-1-methyl-1H-indol-3-yl)-3-methyl-5-oxopentanoic acid (**ω1-OH-197**).* **33** (50.6 mg, 0.0897 mmol) was dissolved in THF (0.5 mL), followed by the addition of LiOH (21.5 mg, 0.897 mmol) in H_2O (0.25 mL). The reaction mixture was stirred at rt for 36 h. The solvents were removed under reduced pressure, and 1 N HCl (2 mL) was added at 0 °C dropwise. The slurry was extracted with EtOAc (4 × 5 mL). The combined organic extracts were washed with brine (15 mL), dried over Na_2SO_4, and the solvents were evaporated under reduced pressure to afford the crude product, which was purified using silica gel column chromatography (60% EtOAc/hexane) to afford the desired product **ω1-OH-197** (25.6 mg, 70%) as a pair of diastereomers. HRMS (ESI) *m/z* calcd for $[C_{22}H_{30}ClNO_4 + H]^+$, 408.1936; found 408.1521.

Synthesis of ω2-OH-197

*Methyl (E)-5-(5-chloro-1-methyl-1H-indol-2-yl)pent-4-enoate (**35**).* To a stirred suspension of (3-carboxypropyl)triphenylphosphonium bromide (**34**) (5.608 g, 13.063 mmol) in THF (30 mL) was added *t*BuOK (25 mL, 1.0 M solution in THF) at –78 °C. After stirring the mixture at rt for 30 min, **4** (1.653 g, 8.537 mmol) in THF (20 mL) was added at –78 °C. The reaction mixture was stirred at rt for 3.5 h. Aqueous NH_4Cl solution (60 mL) was added at rt and the two layers were separated. The aqueous layer was extracted with CH_2Cl_2 (3 x 40 mL), which was washed with brine (100 mL) and dried over Na_2SO_4. The solvents were evaporated, the resulting brown viscous crude product was filtered through Celite 545 and silica, and the solid residue was washed thoroughly with CH_2Cl_2. The filtrates were combined and concentrated to obtain the yellow solid (7.793 g), which was dissolved in DMSO (160 mL) to which was added KOH pellets (1.210 g, 21.566 mmol) at rt. After stirring the mixture for 45 min, CH_3I (1.1 mL, 17.669 g) was added. The reaction mixture was stirred at rt for 4 h. Aqueous NH_4Cl solution (60 mL) was added and the aqueous layer was extracted with Et_2O (3 x 35 mL), the combined organic extracts were washed with brine (2 x 50 mL), dried over Na_2SO_4, concentrated and purified using silica gel column chromatography (15% EtOAc/hex) to obtain **35** as a yellow solid (2.014 g, 85% over two steps). HRMS (ESI) *m/z* calcd for $[C_{15}H_{16}ClNO_2 + H]^+$, 278.0948; found 278.0531. ^{1}H NMR (400 MHz, $CDCl_3$)**:** δ 7.49 (d, *J* = 1.3 Hz, 1H), 7.16 (d, *J* = 1.3 Hz, 1H), 7.09 (dd, *J* = 8.7 Hz, 1.6 Hz, 1H), 6.51 – 6.46 (m, 2H), 6.29 (dt, *J* = 15.6 Hz, 6.8 Hz, 1H), 3.70 (s, 3H), 3.69 (s, 3H), 2.63 – 2.57 (m, 2H), 2.55 – 2.51(m, 2H). ^{13}C NMR ($CDCl_3$): δ 171.5, 137.7, 134.3, 130.9, 127.1, 123.6, 119.8, 118.0, 117.7, 108.3, 96.0, 50.0, 31.8. 28.3, 26.9.

*Methyl 5-(5-chloro-1-methyl-1H-indol-2-yl)pentanoate (**36**).* To a stirred solution of **35** (879 mg, 3.165 mmol) in benzene (20 mL) was added palladium (10 wt. % on activated carbon, 81 mg).

H_2 gas was purged in the reaction flask using a H_2 balloon. The reaction mixture was stirred at rt for 3 h. The mixture was filtered through Celite 545, the solid residue washed with CH_2Cl_2, and the combined filtrate was concentrated to afford **36** as a yellow solid (871 mg, 98 %), which was used without any further purification. HRMS (ESI) *m/z* calcd for $[C_{15}H_{18}ClNO_2 + H]^+$, 280.1104; found 280.0625. ^{1}H NMR (400 MHz, $CDCl_3$): δ 7.47 (d, *J* = 1.2 Hz, 1H), 7.14 (d, *J* = 8.6 Hz, 1H), 7.08 (dd, *J* = 8.6 Hz, 1.7 Hz, 1H), 6.18 (s, 1H), 3.67 (s, 3H), 3.63 (s, 3H), 2.73 (t, *J* = 6.7 Hz, 2H), 2.38 (t, *J* = 6.7 Hz, 2H), 1.18 – 1.72 (m, 4H). ^{13}C NMR ($CDCl_3$): δ 173.8, 142.1, 135.8, 128.8, 124.9, 120.7, 119.1, 109.7, 98.5, 51.6, 33.8, 29.6, 27.8, 26.5, 24.6.

*Synthesis of 6-(5-chloro-1-methyl-1H-indol-2-yl)-2-methylhexan-2-ol (**37**).* To a stirred solution of **36** (276 mg, 0.987 mmol) in THF (6 mL) was added CH_3MgBr (0.8 mL, 3.0 M solution in Et_2O) at –78 °C. The reaction mixture was then allowed to warm to rt, and stirred for 30 min. Aqueous NH_4Cl solution (10 mL) was added and the aqueous layer was extracted with EtOAc (3 x 10 mL). The combined organic extracts were washed with brine (30 mL), dried over Na_2SO_4, filtered and concentrated. Silica gel column chromatography (20-25% EtOAc/hexanes) afforded **37** as a pale-yellow viscous oil (235 mg, 85%). HRMS (ESI) *m/z* calcd for $[C_{16}H_{22}ClNO + H]^+$, 280.1468; found 280.1395.^{1}H NMR (400 MHz, $CDCl_3$): δ 7.48 (d, *J* = 1.8 Hz, 1H), 7.16 (d, *J* = 8.6 Hz, 1H), 7.08 (dd, *J* = 8.6 Hz, 1.7 Hz, 1H), 6.19 (s, 1H), 3.65 (s, 3H), 2.74 (t, *J* = 7.7 Hz, 2H), 1.77 – 1.70 (m, 2H), 1.56 – 1.48 (m, 4H), 1.22 (s, 6H). ^{13}C NMR ($CDCl_3$): δ 142.6, 135.7, 128.8, 124.9, 120.7, 119.1, 109.6, 98.1, 70.9, 43.6, 29.6, 29.3 (2C), 29.0, 26.9, 24.5.

*5-(5-Chloro-2-(5-hydroxy-5-methylhexyl)-1-methyl-1H-indol-3-yl)-3-methyl-5-oxopentanoic acid (**ω2-OH-197**).* To a stirred solution of **37** (91 mg, 0.325 mmol) in CH_2Cl_2 (3 mL) was added

Me_2AlCl (1.2 mL, 1.0 M solution in hexanes). After stirring the mixture at rt for min, 3-methyl glutaric anhydride (**13**) (167 mg, 1.305 mmol) was added at once, and the reaction mixture was then stirred at rt for 3 h. Aqueous NH_4Cl (3 mL) was added and the aqueous layer was extracted with EtOAc (3 x 3 mL). The combined organic extracts were washed brine (6 mL), dried over Na_2SO_4, the solvents removed, and the crude product purified using silica gel column chromatography (3-4% MeOH/CH_2Cl_2) to afford the desired product (**ω2-OH-197**) as a yellow solid (71 mg, 54%). HRMS (ESI) *m/z* calcd for $[C_{22}H_{30}ClNO_4 + H]^+$, 408.1941; found 408.1579. ^1H NMR (400 MHz, $CDCl_3$): δ 7.96 (s, 1H), 7.24 – 7.21 (m, 2H), 3.71 (s, 3H), 3.29 – 3.13 (m, 2H), 3.06 – 2.93 (m, 2H), 2.79 – 2.70 (m, 1H), 2.49 (dd, *J* = 14.7 Hz, 6.3 Hz, 1H), 2.39 (dd, *J* = 14.8 Hz, 6.5 Hz, 1H), 1.67 – 1.54 (m, 6H), 1.24 – 1.23 (m, 6H), 1.17 (d, *J* = 6.8 Hz, 3H).^{13}C NMR ($CDCl_3$): δ 195.8, 175.0, 150.5, 135.2, 128.1, 127.1, 122.5, 120.7, 113.3, 110.6, 71.3, 48.9, 43.0, 41.1, 29.7, 29.6, 29.3, 29.2, 26.6, 26.2, 24.1, 20.7.

Synthesis of ω1,ω2-diOH-197

*4-(5-Chloro-1-methyl-1H-indol-2-yl)-butyric acid (**40**).* To a stirred suspension of phosphonium salt **38** (4.28 g, 10.32 mmol) in anhydrous CH_2Cl_2 (30 mL) was added *t*BuOK (1.0 M in THF, 25.82 mL, 25.82 mmol) at –78 ^oC under argon. The mixture was stirred for 40 min at rt and then cooled to –78 ^oC, and a solution of **4** (1.0 g, 5.164 mmol) in CH_2Cl_2 (10 mL) was added. The reaction mixture was stirred at rt for 5 h and then quenched with saturated NH_4Cl solution (15 mL), extracted with EtOAc (3 X 20 mL) and the combined organic layers were dried over Na_2SO_4. The solvent was evaporated under reduced pressure and the crude residue **39** was used as such for the next step. To a solution of crude **39** (1.0 g) in anhydrous EtOAc/EtOH (4:1, 12 mL), 10% Pd/C (100 mg) was added and stirred at room temperature under a H_2 atmosphere for

6 h. After completion of the reaction, the mixture was filtered through Celite 545, the solvents removed under reduced pressure and the crude residue was purified by silica gel column chromatography using 45% EtOAc/*n*-hexane to afford **40** as an off-white solid (950 mg, 73%, over two steps). HRMS (ESI) *m/z* calcd for $[C_{13}H_{14}ClNO_2+H]^+$: 252.0791, found 252.0594. ^{1}H NMR (400 MHz, DMSO-d_6): δ 12.11 (s, 1H), 7.47 (s, 1H), 7.40 (d, J = 8.6 Hz,1H), 7.05 (d, J = 8.5 Hz, 1H), 6.21 (s, 1H), 3.66 (s, 3H), 2.76 (t, J = 7.4 Hz, 2H), 2.34 (t, J = 7.1 Hz, 2H), 1.91-1.84 (m, 2H). ^{13}C NMR (DMSO-d_6): δ 174.15, 142.50, 135.53, 128.43, 123.42, 119.91, 118.38, 110.75, 98.15, 32.98, 29.42, 25.38, 23.25.

*4-(5-Chloro-1-methyl-1H-indol-2-yl)butan-1-ol (**41**).* To a stirred solution of **40** (472 mg, 1.875 mmol) in THF (10 mL) was added $LiAlH_4$ (373 mg, 9.829 mmol) at 0 °C over a period of 10 min. The reaction mixture was warmed to rt and stirred for 30 min. The mixture was then cooled to 0 °C and saturated NH_4Cl solution (5 mL) was added, followed by EtOAc (15 mL). The supernatant layer was decanted and the solid residue washed thoroughly with EtOAc. The organic extracts were combined, dried over Na_2SO_4, concentrated, and the product was purified using silica gel column chromatography (50% EtOAc/hex) to yield **41** as a pale-yellow solid (372 mg, 83%). HRMS (ESI) *m/z* calcd for $[C_{13}H_{16}ClNO + H]^+$, 238.0998; found 238.0569. ^{1}H NMR (400 MHz, $CDCl_3$): δ 7.47 (d, J = 1.8 Hz, 1H), 7.15 (d, J = 8.6 Hz, 1H), 7.08 (dd, J = 8.6 Hz, 1.9 Hz, 1H), 6.19 (s, 1H), 3.70 (t, J = 6.3 Hz, 2H), 3.64 (s, 3H), 2.75 (t, J = 7.5 Hz, 2H), 1.85 – 1.76 (m, 2H), 1.74 – 1.66 (m, 2H). ^{13}C NMR ($CDCl_3$): δ 142.4, 135.8, 128.8, 124.9, 120.7, 119.1, 109.7, 98.6, 62.6, 32.3, 29.6, 26.6, 24.7.

*2-(4-Bromobutyl)-5-chloro-1-methyl-1H-indole (**42**).* To a stirred solution of **41** (326 mg, 1.371 mmol) in CH_2Cl_2 (8 mL) was added CBr_4 (504 mg, 1.52 mmol) followed by PPh_3 (395 mg, 1.506 mmol) at rt. The reaction mixture was stirred at rt for 1 h. The CH_2Cl_2 was evaporated under reduced pressure and the resulting residue was purified using silica gel column chromatography (10% EtOAc/hexanes) to obtain **42** as a brown solid (387 mg, 94%). HRMS (ESI) *m/z* calcd for $[C_{13}H_{15}BrClNO + H]^+$, 300.0154; found 300.0110. ^{1}H NMR (400 MHz, $CDCl_3$)**:** δ 7.48 (d, *J* = 1.8 Hz, 1H), 7.16 (d, *J* = 8.6 Hz, 1H), 7.09 (dd, *J* = 8.6 Hz, 1.9 Hz, 1H), 6.20 (s, 1H), 3.67 (s, 3H), 3.46 (t, *J* = 7.5 Hz, 2H), 2.73 (t, *J* = 6.5 Hz, 2H), 2.03 – 1.96 (m, 2H), 1.93 – 1.85 (m, 2H). ^{13}C NMR ($CDCl_3$): δ 141.7, 135.8, 128.8, 125.0, 120.9, 119.2, 109.7, 98.8, 33.4, 32.1, 29.7, 26.9, 26.0.

*Diethyl 2-(4-(5-chloro-1-methyl-1H-indol-2-yl)butyl)malonate (**44**).* To a stirred suspension of NaH (30 mg, 60% dispersion in mineral oil) in THF (3 mL) was added diethyl malonate (**43**) (160 μL, 1.049 mmol) at 0 °C. After stirring the mixture at rt for 30 min, a solution of **42** (246 mg, 0.818 mmol) in THF (10 mL) was added at 0 °C. The reaction mixture was allowed to warm to rt and then refluxed gently (at 70 °C) for 14 h. H_2O (10 mL) was added, and the aqueous layer was extracted with EtOAc (3 x 10 mL). The EtOAc extract was dried over Na_2SO_4, concentrated, and the product purified using silica gel column chromatography (10% EtOAc/hex) to yield **44** as a yellow viscous oil (221 mg, 74%). HRMS (ESI) *m/z* calcd for $[C_{20}H_{26}ClNO_4 + H]^+$, 380.1628; found 380.1049. ^{1}H NMR (400 MHz, $CDCl_3$)**:** δ 7.47 (d, *J* = 1.8 Hz, 1H), 7.15 (d, *J* = 8.6 Hz, 1H), 7.08 (dd, *J* = 8.6 Hz, 1.9 Hz, 1H), 6.17 (s, 1H), 4.23 – 4.15 (m, 4H), 3.64 (s, 3H), 3.33 (t, *J* = 7.5 Hz, 1H), 2.73 (t, *J* = 7.6 Hz, 2H), 2.00 – 1.94 (m, 2H), 1.80 – 1.72 (m, 2H), 1.51

– 1.43 (m, 2H), 1.26 (t, *J* = 7.1Hz, 6 H). ^{13}C NMR ($CDCl_3$): δ 169.5 (2 C), 142.2, 135.8, 128.8, 124.9, 120.7, 119.1, 109.7, 98.5, 69.4 (2C), 51.9, 29.6, 28.5, 28.0, 27.0, 26.5, 14.1 (2C).

*2-(4-(5-Chloro-1-methyl-1H-indol-2-yl)butyl)propane-1,3-diol (**45**).* To a stirred solution of **44** (172 mg, 0.470 mmol) in THF (5 mL) was added $LiAlH_4$ (73 mg, 1.924 mmol) at 0 °C over a period of 2 min. The reaction mixture was allowed to warm to rt and stirred for 4 h. The mixture was cooled to 0 °C and saturated aqueous NH_4Cl (2 mL) was added, followed by EtOAc (5 mL). The supernatant layer was decanted and the solid residue was washed thoroughly with EtOAc. The organic extracts were combined, dried over Na_2SO_4, concentrated, and purified using silica gel column chromatography (75% EtOAc/hex) to afford **45** as pale-yellow solid (113 mg, 81%). HRMS (ESI) *m/z* calcd for $[C_{16}H_{22}ClNO_2 + H]^+$, 296.1417; found 296.0787. ^{1}H NMR (400 MHz, $CDCl_3$): δ 7.48 (d, *J* = 1.8 Hz, 1H), 7.16 (d, *J* = 8.6 Hz, 1H), 7.09 (dd, *J* = 8.6 Hz, 1.9 Hz, 1H), 6.18 (s, 1H), 3.85 – 3.81 (m, 2H), 3.71 – 3.67 (m, 2H), 3.65 (s, 3H), 2.73 (t, *J* = 7.7 Hz, 2H), 2.08 (t, *J* = 5 Hz, 2H), 1.83 – 1.70 (m, 3H), 1.52 – 1.45 (m, 2H), 1.37 – 1.32 (m, 2H). ^{13}C NMR ($CDCl_3$): δ 141.0, 137.3, 127.8, 120.6, 119.7, 119.2, 108.7, 98.8, 66.6 (2 C), 42.0, 29.5, 28.8, 27.6, 27.0, 26.7.

*5-(5-chloro-2-(6-hydroxy-5-(hydroxymethyl)hexyl)-1-methyl-1H-indol-3-yl)-3-methyl-5-oxopentanoic acid (**ω1,ω2-diOH-197**).* To a stirred solution of **45** (36 mg, 0.122 mmol) in CH_2Cl_2 (5 mL) was added Me_2AlCl (0.1 mL, 1.0 M solution in hexanes) and the mixture was stirred at rt for a further 20 min. A solution of **10** (20 mg, 0.112 mmol) in CH_2Cl_2 (2 mL) was then added and the reaction mixture stirred at rt for 45 min. Saturated aqueous NH_4Cl (3 mL) was added and the aqueous layer was extracted with CH_2Cl_2 (3 x 5 mL). The combined organic

extracts were dried over Na_2SO_4, filtered, and the solvent removed under reduced pressure to obtain crude **46** (28 mg), which was used without any further purification. A solution of crude **46** (28 mg), $LiOH.H_2O$ (51 mg, 1.215 mmol), THF (1.6 mL), H_2O (4.5 mL), and MeOH (2 drops) were mixed together, and stirred at rt for 22 h. H_2O (6 mL). Aqueous HCl (0.1 mL, 4.26 M) was added and the aqueous layer was extracted with EtOAc (3 x 4 mL). The combined organic extracts were washed with brine (8 mL), dried over Na_2SO_4, concentrated to dryness, and the residue was purified using silica gel column chromatography (10-15% MeOH/CH_2Cl_2) to yield the desired product (**ω1,ω2-diOH-197**) as a yellow viscous oil (28 mg, 59% over two steps). HRMS (ESI) *m/z* calcd for $[C_{22}H_{30}ClNO_5 + H]^+$, 424.1891; found 424.1613. ^{1}H NMR (400 MHz, $CDCl_3$)**:** δ 7.98 (s, 1H), 7.24 – 7.21 (m, 2H), 3.89 – 3.84 (m, 2H), 3.74 – 3.66 (m, 5H), 3.15 – 2.95 (m, 3H), 2.78 – 2.66 (m, 1H), 2.42 – 2.40 (m, 2H), 1.92 – 1.90 (m, 1H), 1.69 – 1.33 (m, 7H), 1.17 (d, J = 6.8 Hz, 3H). ^{13}C NMR ($CDCl_3$): δ 195.6, 174.8, 150.4, 135.2, 128.1, 127.1, 122.5, 120.7, 113.2, 110.6, 66.6, 66.4, 49.2, 40.9, 29.7 (2C), 28.7, 26.6 (2C), 26.5, 26.0, 21.1.

Synthesis of dinor-ω-CO_2H-230

*4-(5-Chloro-1-methyl-1H-indol-2-yl)-butyric acid methyl ester (**47**).* To a solution of **40** (900 mg, 3.51 mmol) in anhydrous DMSO (5 mL) was added KOH (401 mg, 7.15 mmol) at 0 ^{o}C under argon. The reaction mixture was stirred for 45 min at room temperature followed by addition of methyl iodide (445 mg, 7.15 mmol). Stirring was continued for 4 h and then the mixture was quenched with saturated aqueous NH_4Cl (6 mL), extracted with EtOAc (4 x 10 mL) and the combined organic layers were dried over Na_2SO_4. The solvent was evaporated under reduced pressure and the crude residue was purified by silica gel column chromatography using 25% EtOAc/*n*-hexane to yield **47** as colorless liquid (807 mg, 80%). HRMS (ESI) *m/z* calcd for

$[C_{14}H_{16}ClNO_2+H]^+$: 266.0948, found 266.0948. ^{1}H NMR (400 MHz, $CDCl_3$): 7.47 (d, *J* = 1.6 Hz,1H), 7.15 (d, *J* = 8.6 Hz, 1H), 7.09 (dd, *J* = 8.6, 1.8 Hz, 1H), 6.19 (s, 1H), 3.66 (s, 3H), 3.65 (s, 3H), 2.77 (t, *J* = 5.6 Hz, 2H), 2.4 (t, *J* = 7.2Hz, 2H), 2.08-1.99 (m, 2H).^{13}C NMR ($CDCl_3$): δ 172.5, 140.2, 134.7, 127.6, 123.8, 119.8, 118.1, 108.6, 97.8, 50.5, 32.1, 28.5, 25.0, 22.5.

*Synthesis of 5-[5-Chloro-2-(3-methoxycarbonyl-propyl)-1-methyl-1H-indol-3-yl]-3-methyl-5-oxo-pentanoic acid methyl ester (**48**).* To a stirred solution of **47** (700 mg, 2.63 mmol) in CH_2Cl_2 (20 mL) was added Me_2AlCl (1.0 M in hexane, 5.26 mL, 5.26 mmol) at rt and the mixture was stirred for a further 30 min. A solution of **10** (564 mg, 3.16 mmol) in CH_2Cl_2 (12 mL) was then added and stirring was continued at rt for 30 min. The reaction mixture was quenched by adding saturated aqueous NH_4Cl (8 mL) and the organic layer was extracted with CH_2Cl_2 (3 x 20 mL). The combined organic layers were washed with brine (5 mL) and dried over Na_2SO_4. The solvents were evaporated under reduced pressure and the crude product was purified by silica gel column chromatography using 30% EtOAc/*n*-Hex to afford **48** as a colorless viscous liquid (440 mg, 41%). HRMS (ESI) *m/z* calcd for $[C_{21}H_{26}ClNO_5 + H]^+$: 408.1578, found 408.1059. ^{1}H NMR (400 MHz, $CDCl_3$): δ 7.85 (d, *J* = 1.4 Hz, 1H), 7.26 (d, *J* = 2.1Hz, 1H), 7.23 (d, *J* = 1.7 Hz, 1H), 3.76 (s, 3H), 3.68 (s, 3H), 3.66 (s, 3H), 3.24 (t, *J* = 5.8 Hz, 2H) 3.03 (dd, *J* = 16. 2, 6.4 Hz, 1H), 2.90 (dd, *J* = 16.2, 7.0 Hz, 1H), 2.78 – 2.66 (m, 1H), 2.55 – 2.48 (m, 3H), 2.32 (dd, *J* = 14.9, 7.6 Hz, 1H), 1.19 – 1.90 (m 2H), 1.10 (d, *J* = 6.6, Hz, 3H). ^{13}C NMR ($CDCl_3$): δ 195.0, 173.9, 173.2, 149.5, 135.2, 128.8, 127.9, 122.4, 120.3, 113.5, 110.8, 51.61, 51.5, 49.4, 41.1, 33.1, 29.7, 26.4, 25.4, 23.7, 20.3.

*5-[2-(3-Carboxy-propyl)-5-chloro-1-methyl-1H-indol-3-yl]-3-methyl-5-oxo-pentanoic acid (**dinor-ω-CO_2H-230**).* To a stirred solution of **48** (300 mg, 0.73 mmol) in THF (20 mL) and H_2O (5 mL) was added LiOH (352 mg, 14.72 mmol) and the mixture was stirred at rt for 24 h, after which time the solvents were evaporated to dryness under reduced pressure. The resulting residue was dissolved in H_2O (12 mL), and, after cooling to 0 ^oC, 6 N HCl (4.8 mL) was added dropwise (pH = 3). After extraction with EtOAc (3 X 20 mL), the combined organic layers were washed with brine (7 mL) and dried over anhydrous Na_2SO_4. The solvents were evaporated under reduced pressure to obtain the crude product, which was purified by silica gel column chromatography using 80% EtOAc/*n*-Hex to afford **dinor-ω-CO_2H-230** as an off-white solid (184 mg, 66%). HRMS (ESI) *m/z* calcd for $[C_{19}H_{22}ClNO_5 + H]^+$: 380.1265, found 380.1047. ^{1}H NMR (400 MHz, CD_3COCD_3): δ 10.43 (br s, 2H), 7.92 (d, *J* = 1.7 Hz, 1H), 7.38 (d, *J* = 8.7 Hz, 1H), 7.09 (dd, *J* = 8.7, 1.9 Hz, 1H), 3.74 (s, 3H), 3.17 (t, *J* = 8.0 Hz, 2H), 2.99 (dd, *J* = 16. 4, 6.0 Hz, 1H), 2.85 (dd, *J* = 16.5, 7.3 Hz, 1H), 2.62 – 2.52 (m, 1H), 2.45 – 2.36 (m, 3H), 2.17 (dd, *J* = 15.4, 8.0 Hz, 1H), 1.87-1.78 (m, 2H), 0.96 (d, *J* = 6.6, Hz, 3H). ^{13}C NMR (CD_3COCD_3): δ 195.3, 174.4, 174.0, 150.3, 136.4, 128.03, 127.98, 122.8, 121.2, 114.2, 112.4, 49.7, 41.1, 33.5, 30.1, 27.1, 26.1, 24.8, 20.4.

Synthesis of *51*

*5-Chloro-1-methyl-1H-indole (**50**).* To a stirred solution of 5-chloro-indole (**49**) (4.52 g, 29.817 mmol) in DMF (50 mL) was added NaH (1.43 g, 35.6 mmol, 60% dispersion in mineral oil) slowly at 0 °C over a period of 20 min. After 45 min, CH_3I (2.22 mL, 35.6 mmol) was added dropwise at 0 °C. The reaction mixture was stirred at rt for 18 h. The reaction was quenched with the addition of saturated aqueous NH_4Cl (100 mL) at 0 °C. The aqueous layer was extracted with

Et_2O (3 × 150 mL), which was then washed with brine (2 × 100 mL), dried over Na_2SO_4, and the solvents removed *in vacuo* to obtain crude **50** as a yellow solid (4.62 g, 94%), which was used without any further purification. HRMS (ESI) *m/z* calcd for $[C_9H_8ClN + H]^+$, 166.0418; found 166.0256. ^{1}H NMR (400 MHz, $CDCl_3$): δ 7.58 (d, *J* = 1.9 Hz, 1H), 7.24 – 7.21 (m, 1H), 7.16 (dd, *J* = 8.7, 1.9 Hz, 1H), 7.06 (d, *J* = 3.1Hz, 1H), 6.42 (dd, *J* = 3.1, 0.9 Hz, 1H), 3.78 (s, 3H). ^{13}C NMR ($CDCl_3$): δ 135.11, 130.08, 129.41, 125.09, 121.78, 120.18, 110.17, 100.60, 33.02.

*5-(5-Chloro-1-methyl-1H-indol-3-yl)-3-methyl-5-oxopentanoic acid (**51**).* To a stirred solution of **50** (1.28 g, 7.729 mmol) in CH_2Cl_2 (3 mL) was added Me_2AlCl (30.0 mL, 1.0 M solution in hexanes) dropwise at 0 °C. After 30 min, 3-methylglutaric anhydride (**13**) (5.95 g, 46.437 mmol) was added in a single portion at rt, and the reaction mixture was stirred at rt for 3 h. Saturated NH_4Cl solution (4 mL) was added at 0 °C, and the organic layer was extracted with EtOAc (3 × 5 mL), the combined organic extracts were washed with brine (20 mL), dried over Na_2SO_4, and the solvents were evaporated to obtain the crude product, which was purified using silica gel column chromatography (10% MeOH in CH_2Cl_2) to yield **51** as an off-white solid (1.83 g, 81%). $[C_{15}H_{16}ClNO_3 + H]^+$, 294.0891; found 294.0322. ^{1}H NMR (400 MHz, $CDCl_3$): δ 8.41 (d, *J* = 1.8 Hz, 1H), 7.79 (s, 1H), 7.27 (m, 2H), 3.85 (s, 3H), 2.96 (dd, *J* = 14.3, 6.1Hz, 1H), 2.69 (ddd, *J* = 27.2, 13.9, 7.0 Hz, 2H), 2.54 – 2.30 (m, 2H), 1.11 (d, *J* = 6.5 Hz, 3H). ^{13}C NMR ($CDCl_3$): δ 194.52, 177.11, 136.63, 135.87, 128.85, 127.28, 123.92, 122.27, 116.22, 110.66, 45.79, 40.79, 33.79, 27.84, 20.2.

Ancillary Information

Corresponding Author Information:

William S. Powell, Meakins-Christie Laboratories, Centre for Translational Biology, McGill University Health Centre, 1001 Decarie Blvd, Montreal, QC H4A 3J1, Canada; Telephone: 514-934-1934 ext. 76414; email: william.powell@mcgill.ca

Present Address

[⊥] ***Vivek Gore****:* Navinta LLC, 1499 Lower Ferry Rd, Ewing, New Jersey 08618-1414, USA

Author Contributions:

[‖] *Chantal Cossette and Shishir Chourey* contributed equally to this work

***Acknowledgments*:**

This work was supported by the Canadian Institutes of Health Research (Grants MOP-6254 and PP2-133388), the American Asthma Foundation (Grant 12-0049), and the National Heart, Lung, and Blood Institute (Grant R01HL081873) and by AmorChem (Montreal, QC). The Meakins-Christie Laboratories-MUHC-RI are supported in part by a Centre grant from Le Fond de la Recherche en Santé du Québec as well as by the J. T. Costello Memorial Research Fund. J.R. also wishes to acknowledge the National Science Foundation for the AMX-360 (Grant CHE-90-13145) and Bruker 400 MHz (Grant CHE-03-42251) NMR instruments. D.V. and I.S. were supported by the Natural Sciences and Engineering Research Council of Canada (Grant RGPIN/435814-2103). I.S. also wishes to acknowledge the Centre for Biological Applications of Mass Spectrometry at Concordia University for PhD scholarship funding. The content is solely

the responsibility of the authors and does not necessarily represent the official views of the National Heart, Lung, and Blood Institute or the National Institutes of Health.

Abbreviations Used:

5-HEDH, 5-hydroxyeicosanoid dehydrogenase; 5-HETE, 5S-hydroxy-6E,8Z,11Z,14Z-eicosatetraenoic acid; 5-oxo-ETE, 5-oxo-6E,8Z,11Z,14Z-eicosatetraenoic acid; DHP, dihydropyran; DMF, dimethylformamide; DMP, Dess-Martin Periodane; DMSO, dimethylsulfoxide; HRMS, high resolution mass spectrometry; LT, leukotriene; MeCN, acetonitrile; MeOH, methanol; NBD-phallacidin, N-(7-nitrobenz-2-oxa-1,3-diazol-4-yl)phallacidin; PBS, phosphate-buffered saline; PMA, phorbol 12-myristate 13-acetate; PPTS, pyridinium *p*-toluenesulfonate; TMS, tetramethylsilane.

References

1. Powell, W. S.; Rokach, J. The eosinophil chemoattractant 5-oxo-ETE and the OXE receptor. *Prog. Lipid Res.* **2013,** *52*, 651-665.

2. Jones, C. E.; Holden, S.; Tenaillon, L.; Bhatia, U.; Seuwen, K.; Tranter, P.; Turner, J.; Kettle, R.; Bouhelal, R.; Charlton, S.; Nirmala, N. R.; Jarai, G.; Finan, P. Expression and characterization of a 5-oxo-6E,8Z,11Z,14Z-eicosatetraenoic acid receptor highly expressed on human eosinophils and neutrophils. *Mol. Pharmacol.* **2003,** *63*, 471-477.

3. Monneret, G.; Gravel, S.; Diamond, M.; Rokach, J.; Powell, W. S. Prostaglandin D_2 is a potent chemoattractant for human eosinophils that acts via a novel DP receptor. *Blood* **2001,** *98*, 1942-1948.

4. Sun, F. F.; Crittenden, N. J.; Czuk, C. I.; Taylor, B. M.; Stout, B. K.; Johnson, H. G. Biochemical and functional differences between eosinophils from animal species and man. *J. Leukoc. Biol.* **1991,** *50*, 140-150.

5. Gore, V.; Gravel, S.; Cossette, C.; Patel, P.; Chourey, S.; Ye, Q.; Rokach, J.; Powell, W. S. Inhibition of 5-oxo-6,8,11,14-eicosatetraenoic acid-induced activation of neutrophils and eosinophils by novel indole OXE receptor antagonists. *J. Med. Chem.* **2014,** *57*, 364-377.

6. Patel, P.; Reddy, C. N.; Gore, V.; Chourey, S.; Ye, Q.; Ouedraogo, Y. P.; Gravel, S.; Powell, W. S.; Rokach, J. Two Potent OXE-R Antagonists: Assignment of Stereochemistry. *ACS Med. Chem. Lett.* **2014,** *5*, 815-819.

7. Enyedi, B.; Kala, S.; Nikolich-Zugich, T.; Niethammer, P. Tissue damage detection by osmotic surveillance. *Nat. Cell Biol.* **2013,** *15*, 1123-1130.

8. Cossette, C.; Gravel, S.; Reddy, C. N.; Gore, V.; Chourey, S.; Ye, Q.; Snyder, N. W.; Mesaros, C. A.; Blair, I. A.; Lavoie, J. P.; Reinero, C. R.; Rokach, J.; Powell, W. S. Biosynthesis and actions of 5-oxoeicosatetraenoic acid (5-oxo-ETE) on feline granulocytes. *Biochem. Pharmacol.* **2015,** *96*, 247-255.

9. Powell, W. S.; Wang, L.; Khanapure, S. P.; Manna, S.; Rokach, J. High-pressure liquid chromatography of oxo-eicosanoids derived from arachidonic acid. *Anal. Biochem.* **1997,** *247*, 17-24.

10. Powell, W. S.; Gravelle, F.; Gravel, S. Phorbol myristate acetate stimulates the formation of 5-oxo-6,8,11,14-eicosatetraenoic acid by human neutrophils by activating NADPH oxidase. *J. Biol. Chem.* **1994,** *269*, 25373-25380.

11. Pawlowski, N. A.; Kaplan, G.; Hamill, A. L.; Cohn, Z. A.; Scott, W. A. Arachidonic acid metabolism by human monocytes. Studies with platelet-depleted cultures. *J. Exp. Med.* **1983,** *158*, 393-412.

12. Powell, W. S.; Gravel, S.; Halwani, F.; Hii, C. S.; Huang, Z. H.; Tan, A. M.; Ferrante, A. Effects of 5-oxo-6,8,11,14-eicosatetraenoic acid on expression of CD11b, actin polymerization and adherence in human neutrophils. *J. Immunol.* **1997,** *159*, 2952-2959.

13. Powell, W. S.; Gravel, S.; MacLeod, R. J.; Mills, E.; Hashefi, M. Stimulation of human neutrophils by 5-oxo-6,8,11,14- eicosatetraenoic acid by a mechanism independent of the leukotriene B_4 receptor. *J. Biol. Chem.* **1993,** *268*, 9280-9286.

14. Kundu, R. K.; Getz, G. S.; Tonsgard, J. H. Induction of (omega-1)-oxidation of monocarboxylic acids by acetylsalicylic acid. *J. Lipid Res.* **1993,** *34*, 1187-1199.

15. Kikuta, Y.; Kusunose, E.; Okumoto, T.; Kubota, I.; Kusunose, M. Purification and characterization of two forms of cytochrome P-450 with omega-hydroxylase activities toward prostaglandin A and fatty acids from rabbit liver microsomes. *J. Biochem.* **1990,** *107*, 280-286.

16. Theoharides, A. D.; Kupfer, D. Evidence for different hepatic microsomal monooxygenases catalyzing omega- and (omega-1)-hydroxylations of prostaglandins E_1 and E_2. Effects of inducers of monooxygenase on the kinetic constants of prostaglandin hydroxylation. *J. Biol. Chem.* **1981,** *256*, 2168-2175.

17. Romano, M. C.; Eckardt, R. D.; Bender, P. E.; Leonard, T. B.; Straub, K. M.; Newton, J. F. Biochemical characterization of hepatic microsomal leukotriene B_4 hydroxylases. *J. Biol. Chem.* **1987,** *262*, 1590-1595.

18. Farley, S. M.; Leonard, S. W.; Taylor, A. W.; Birringer, M.; Edson, K. Z.; Rettie, A. E.; Traber, M. G. omega-Hydroxylation of phylloquinone by CYP4F2 is not increased by alpha-tocopherol. *Mol. Nutr. Food Res.* **2013,** *57*, 1785-1793.

19. Parker, R. S.; Sontag, T. J.; Swanson, J. E.; McCormick, C. C. Discovery, characterization, and significance of the cytochrome P450 omega-hydroxylase pathway of vitamin E catabolism. *Ann. N. Y. Acad. Sci.* **2004,** *1031*, 13-21.

20. Hamman, M. A.; Thompson, G. A.; Hall, S. D. Regioselective and stereoselective metabolism of ibuprofen by human cytochrome P450 2C. *Biochem. Pharmacol.* **1997,** *54*, 33-41.

21. Bardowell, S. A.; Duan, F.; Manor, D.; Swanson, J. E.; Parker, R. S. Disruption of mouse cytochrome p450 4f14 (Cyp4f14 gene) causes severe perturbations in vitamin E metabolism. *J. Biol. Chem.* **2012,** *287*, 26077-26086.

22. Reddy, C. N.; Ye, Q. J.; Chourey, S.; Gravel, S.; Powell, W. S.; Rokach, J. Stereoselective synthesis of two highly potent 5-oxo-ETE receptor antagonists. *Tetrahedron Lett.* **2015,** *56*, 6896-6899.

23. Weerawarna, S. A.; Geisshusler, S. M.; Murthy, S. S.; Nelson, W. L. Enantioselective and diastereoselective hydroxylation of bufuralol. Absolute configuration of the 7-(1-hydroxyethyl)-2-[1-hydroxy-2-(tert-butylamino)ethyl]benzofurans, the benzylic hydroxylation metabolites. *J. Med. Chem.* **1991,** *34*, 3091-3097.

24. Lindeke, B.; Ericsson, O.; Jonsson, A.; Noren, B.; Stromberg, S.; Vangbo, B. Biotransformation of terodiline. III. Opposed stereoselectivity in the benzylic and aromatic hydroxylations in rat liver microsomes. *Xenobiotica* **1987,** *17*, 1269-1278.

25. Zollner, A.; Dragan, C. A.; Pistorius, D.; Muller, R.; Bode, H. B.; Peters, F. T.; Maurer, H. H.; Bureik, M. Human CYP4Z1 catalyzes the in-chain hydroxylation of lauric acid and myristic acid. *Biol. Chem.* **2009,** *390*, 313-317.

26. Carroll, M. A.; Balazy, M.; Huang, D. D.; Rybalova, S.; Falck, J. R.; McGiff, J. C. Cytochrome P450-derived renal HETEs: storage and release. *Kidney Int.* **1997,** *51*, 1696-1702.

27. Powell, W. S. Precolumn extraction and reversed-phase high-pressure liquid chromatography of prostaglandins and leukotrienes. *Anal. Biochem.* **1987,** *164*, 117-131.

28. Kay, A. B. Studies on eosinophil leucocyte migration. II. Factors specifically chemotactic for eosinophils and neutrophils generated from guinea-pig serum by antigen-antibody complexes. *Clin. Exp. Immunol.* **1970,** *7*, 723-737.

29. Powell, W. S. Rapid extraction of oxygenated metabolites of arachidonic acid from biological samples using octadecylsilyl silica. *Prostaglandins* **1980,** *20*, 947-957.

30. Yadav, V. K.; Fallis, A. G. Regioselective cleavage of 2-methyltetrahydrofuran - a versatile synthesis of 1-halo-4-pentanols and 4-halo-1-pentanols. *J. Org. Chem.* **1986,** *51*, 3372-3374.

31. Sabitha, G.; Fatima, N.; Gopal, P.; Reddy, C. N.; Yadav, J. S. Stereoselective total synthesis of (+)-strictifolione and (6R)-6-[(4R,6R)-4,6-dihydroxy-10-phenyldec-1-enyl]-5,6-dihydro-2H-pyran-2-one by Prins reaction and olefin cross-metathesis. *Tetrahedron-Asymmetry* **2009,** *20*, 184-191.

32. Cheng, H. Y.; Lin, Y. S.; Sun, C. S.; Shih, T. W.; Tsai, H. H. G.; Hou, D. R. Ring-closing metathesis and palladium-catalyzed formate reduction to 3-methyleneoxepanes. Formal synthesis of (-)-zoapatanol. *Tetrahedron* **2012,** *68*, 747-753.

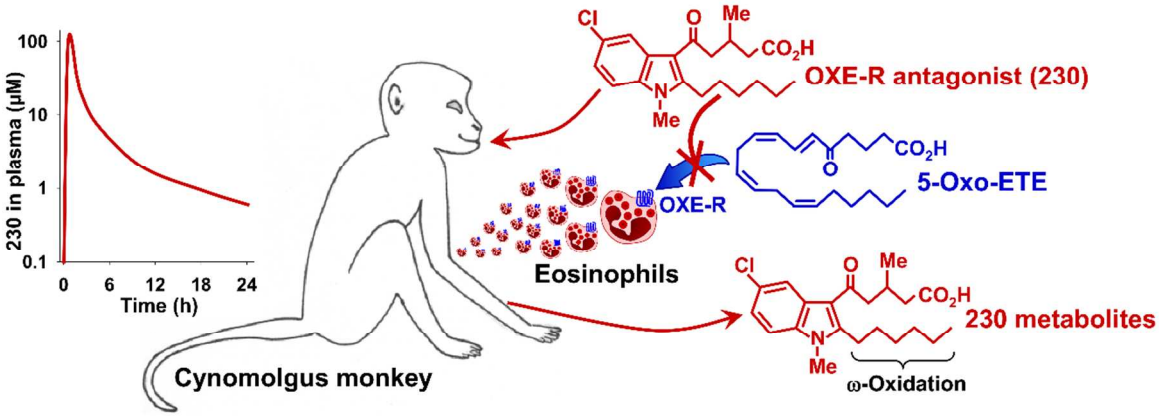

Table of Contents graphic